University of Nottingham

School of Mathematical Sciences

A thesis submitted in fulfillment of the requirements of a MPhil degree in mathematics

Communication through complex media: a novel interdisciplinary paradigm to bridge information theory and multi-scale flow and transport theory

Supervisors:
Dr. Matteo Icardi
Dr. Gabriele Gradoni

Author:
John Couch

November 2021

Abstract

Molecular communication (MC) is a relatively new type of communication which makes use of particles to transmit information. The movement towards particle transfer is appealing as it broadens the range of what we can communicate through (more) efficiently, such as porous mediums. The applications of MC systems are vast, ranging from medical treatments to industrial problems. In this thesis, we combine fluid mechanics and communication theory with the aim to understand MC in a mathematical framework. This approach is still in its infancy, progressing the idea of combining these two fields, providing a solid mathematical basis which can be used for future research in information transfer. In an effort to step further into work done on the study of transport models, specifically work which took the fluid mechanical perspective of studying transport models, an extension is put forward; introducing ideas from communication theory such as transmission, modulation, reception, and demodulation, to find an optimal way of sending information across a porous medium. We begin here, rethinking what it might mean to have a general modulating function; the idea of allowing for a negative (concentration) signal to transmit information opens up the possibility of using functions which are not used in molecular communication as of yet. This gives rise to the novelty of this report, which is the use of biorthogonal functions. We use a generic transfer function and make use of both the modulating- and demodulating- functions. These functions lead to the idea of using orthogonality conditions to help in the optimization process. The idea of combining transport models with communication theory has the potential to open new avenues of research. We believe this can lead to promising results in the future for molecular communication, and perhaps communication in general.

Contents

1 Introduction **1**
- 1.1 Transport theory and communication theory . . . 2
- 1.2 Transport models . . . 6

2 Modulation **8**
- 2.1 Simple Modulation . . . 9
  - 2.1.1 Communication framework . . . 10
  - 2.1.2 Channel model: Delta function . . . 13
  - 2.1.3 Channel model: ADE . . . 14
- 2.2 Generic Modulation . . . 18
  - 2.2.1 Modulation-Demodulation scheme in discrete time . . . 19
  - 2.2.2 Singular Value Decomposition of The Transfer Function . . . 20
  - 2.2.3 Optimising signal error . . . 22

3 Conclusion **26**

4 Appendix **27**
- 4.1 Models and results . . . 27
  - 4.1.1 Advection-Diffusion Transfer Function . . . 27
  - 4.1.2 Mobile-Immbile Transfer Function . . . 29
  - 4.1.3 Multi-Phase Flow Model . . . 32
  - 4.1.4 Multi-Rate-Mass-Transfer Model . . . 33
  - 4.1.5 Towards uncertainty quantification: sensitivity analysis . . . 33
- 4.2 Methods and Proofs . . . 34
  - 4.2.1 Proof of THM 1 . . . 34
  - 4.2.2 A procedural approach . . . 35
  - 4.2.3 Fourier in time (and space?) . . . 37
  - 4.2.4 3D code . . . 39
  - 4.2.5 Oscillatory channel . . . 39
  - 4.2.6 Expansion of $\tilde{\phi}_j$ . . . 41
- 4.3 Singular Value Decomposition . . . 43
  - 4.3.1 Reduced SVD . . . 43

1 Introduction

Molecular communication (MC) is a relatively new way of thinking about information transfer, moving from encoding a signal onto a wave-packet to encoding information onto particles. Modern day science solves the problem of transmitting information over some distance by encoding the information into wave-form sinusoidal functions which are then used to carry the signal. This approach to information transfer is well studied in literature [1, 2, 3, 4, 5] and is very powerful when dealing with problems in electromagnetism to radio-signals. However, it has its limitations in electromagnetic wireless communication inside networks of tunnels, pipelines, and salt-water environments, as pointed out in [6] and references therein, namely [7, 8, 9]. To overcome problems in communication for situations like these we move towards MC. MC is a new paradigm of information transfer inspired by biology, where the study of how cells communicate with one another using chemical signals has been largely investigated [10]. Studies of nature show that MC is used at the nanoscale, microscale, and macroscale, from cells communicating internally (intra-cellular) and externally (inter-cellular) to pheromones being used between members of the same species. This makes MC a sought-after technology, with research growing in recent years to understand further its applications and limitations.

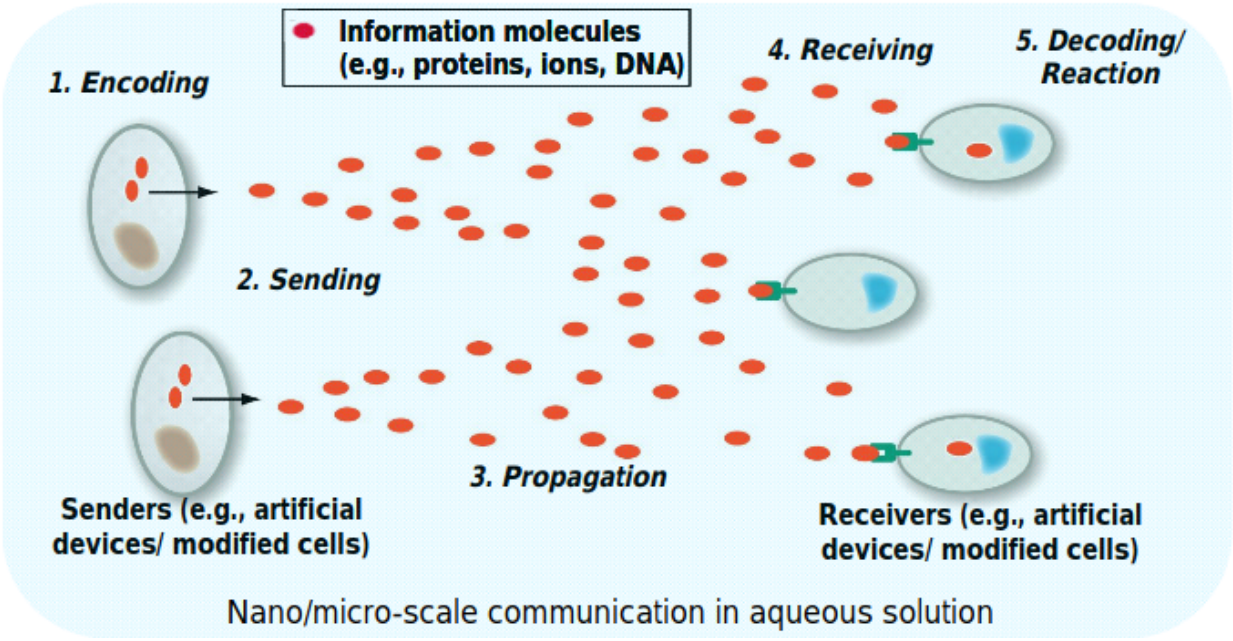

Figure 1: A graphical representation of the whole transmission to reception process present in molecular communication ([11], page 3).

Fig. 1 shows the generic concept of how molecules are transmitted, propagated, and received. This is the framework from which we work, where we transmit our information into a porous medium, have this information propagate through the channel governed by a transfer function, and finally receive this information at the receptors. Note that the extra details such has how we encode this information into the particles, or how we decode and retrieve the information, is not

studied here; this is an open question to be explored in the future.

In this report, we aim to develop a proper mathematical framework that generalises communication metrics for arbitrary information transfer processes. This approach is unique as it offers a different viewpoint of that which is common in literature, providing a solid mathematical basis which can be used for numerical approximations; compared to the usual engineering approach of taking fluid dynamic computational simulations and making numerical approximations from them. The novelty of the approach used in this report is the use of bi-orthogonal functions. For this report we refer to biorthogonal functions as the modulating and demodulating functions. These two functions, denoted as ϕ and $\tilde{\phi}$ respectively, exist in the space of continuous functions $C^0([0,T])$ over some time interval T. They constitute the basis of the mathematical framework we develop in this report.

Throughout this report we assume we have complete knowledge of the channel we send information across, denoted by h. This channel is commonly referred to as the *transfer function* of the system in literature. However, this assumption is not a correct depiction in industry, as knowing the channel in which information is being transferred is not currently possible, so approximations are typically made from models. This is to be discussed further in future work, with research into new ways of approximating a channel to be of potential interest. For now, we will continue with the assumption that we know the transfer function and calculate the optimum communication process by finding an optimal set of modulating and demodulating functions for the given channel. We achieve this using a mathematical tool known as singular value decomposition (SVD), which is performed in discrete time. We measure the efficiency of the communication process by calculating bit error rates (BERs) and observing so called '*waterfall diagrams*' which compare the probability of error in the signal to the noise present in the channel. Noise is a complicated feature in communication which affects how reliable a signal obtained at the receiver is. In our models we choose to take two different types of noise; namely we look at multiplicative noise and additive noise, where a definition and comparison of the two is made. However, we first begin by discussing the importance of transport theory in molecular communication as a motivation for this work, and the literature done in thie field.

1.1 Transport theory and communication theory

Porous media are structures present in all walks of life from naturally formed pockets in rocks or sand, to artificially created pockets in sponges or cake. They are studied in fluid mechanics which generally deals with the study of fluid flow in finite systems. The properties of porous media and their importance in many areas of applied science means they are not just studied in fluid mechanics, but also in biology, biophysics, geoscience, material science, etc. There are many different models which can be studied in these systems, with the vast majority falling under two main branches: incompressible models and compressible models [12, 13].

Research reviews on molecular communication in fluid mechanics has been discussed heavily in literature [11], with its differences in approach and innovative ideas being put forward as the alternative to classical wave communication. State of the art work on molecular communication in the area of transport models gives ample evidence to show its promise as the new method of com-

munication in certain situations. Particularly, research carried out on particulate drug delivery systems [14, 15, 16] provides evidence that molecular communication can be applied to medicine, with transport models related with blood flow used for the human anatomy, and nanonetworks [17, 18, 19, 20, 21, 22, 23]. Other examples such as mass transfer in pore-scale heterogeneous media [24] shows that molecular communication is suitable for describing the removal of dissolved organic compounds from natural porous media. Further studies have looked at how molecular communication can build on classical communication, working in time-frequency domains [25], as well as studies on how noise affects the communication process [26, 27, 28, 29] in molecular communication.

Common transport models which have been studied in the past are advection-diffusion models, where analytical and numerical solutions have been discussed [30, 31], advection-diffusion-reaction models where Galerkin approximations have been made [32], and many more models which have also been applied to molecular communication, such as multi-rate mass transfer models [33]. The model this report focuses on is the advection-diffusion model, with multi-rate mass transfer- and multiphase- flow models being omitted for the time being. These models come under the branch of non-Fickian transport models, and describe both convective and dispersive properties of transport; with the advection-diffusion-reaction model including a reactive transport process [34].

There is also vast amounts of literature focusing more on the communication theory aspects of molecular communication, such as studies on reducing inter-symbol interference (ISI) - a distortion of a signal from one symbol interfering with subsequent symbols. Plenty of research has gone into trying to reduce ISI, inter-Doppler interference (IDI), and inter-carrier interference (ICI) [35]. IDI and ICI are linked via Orthogonal Frequency Division Multiplexing (OFDM) transmissions with frequency offsets and doppler spreads causing interference. Understanding how these interferences behave allows one to improve the efficiency of a system. These studies have provided many results, showing how IDI is present in ideal pulse-shaping waveforms, yet in rectangular waveforms the presence of ICI and ISI is there too [36]. Through use of bi-orthogonal modulating and demodulating functions, we aim to provide a further development on this matter. Although this report does not study IDI and ICI specifically, a brief explanation of what they are is needed to show one motivation behind using biorthogonal functions, as they may be useful in reducing ISI and ICI. This is important due to the work done by [37], which suggests that modern day wireless systems are not limited by additive white Gaussian noise (AWGN), so reducing ISI and ICI is more impactful. This report discusses a few of the challenges in molecular communication, such as symbol optimization [38], where the duration of time between consecutive signals affects the distortion of the signal. There is a diverse number of transport models used in molecular communication and this report, ranging from simple 1D advection-diffusion, to the mobile-immobile model, with the future aim of working with 3D Multi-rate mass transfer models [39, 40].

The novel approach put forward in this report bridges the gap between information theory and fluid mechanics. In the first report, when studying models in fluid mechanics, we used common techniques to obtain transfer functions and breakthrough curves. We now extend this by taking these transfer functions and applying them in a communication setting with a generic modulating/carrier function. We investigate how to efficiently transmit information across a porous medium using biorthogonal functions. In doing so we delve deeper into communication theory,

taking ideas such as transmission, reception, modulation, and demodulation, where we obtain an optimum set of modulating and demodulating functions. These functions yield the optimal solution for sending and retrieving information across a porous medium. To quantify the efficiency of the solution we plot the main results of the report: the waterfall diagrams of bit error rate (BER) vs signal-to-noise-ratio (SNR), which mirror the trajectories of that shown in state-of-the-art literature [41, 42, 43, 44, 45]. Bit error rate is the quantitative measure of how efficient a process is in obtaining bits of information, i.e., how much correct information is received from the original transmitted signal. To calculate BER we need to obtain the ratio between how many bits of information have been received in error to how many bits in total have been received. Signal-to-noise-ratio is the measure of how much noise is present in a system. If this ratio is large then it means there is not much noise in the system, if it is small then it means there is a lot of noise in the system. The transmission of information is considered to be an injection of particles into the porous medium, where the particles have been encoded with the desired information; the channel is considered to be the porous medium in which the particles travel in, defined by a given transfer function, and the receiver is considered to be a location in the porous medium of which the particles pass through. The modulation is associated with the transmission, and the demodulation is associated with the reception.

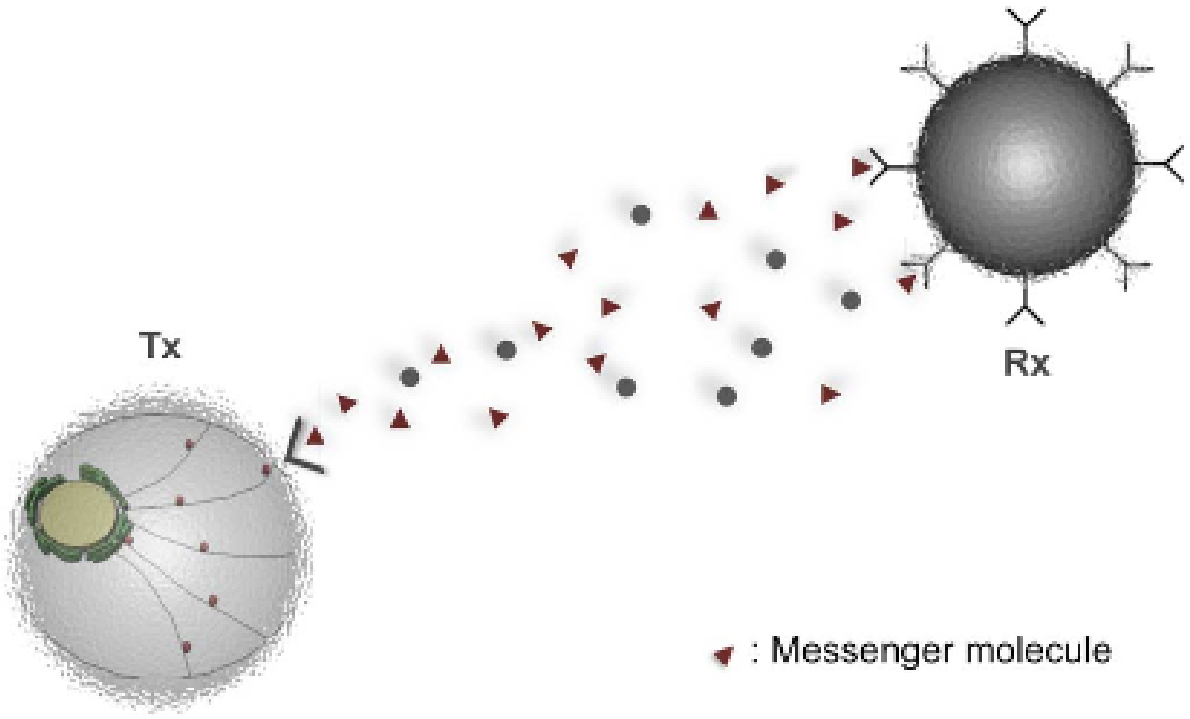

Figure 2: A graphical representation of the presence of noise in the system. As the information propagates throughout the medium to reach the receiver, the presence of the extra information in the medium (the noise), affects the effectiveness of the receiver demodulating the intended signal, as the noise in the system interrupts the process. (N. Kim, A. W. Eckford, and C. Chae. (2014).

Other results discussed in this report are placed in the appendix, as they require future work to be done. A final remark to be made is that throughout this report we talk about modulation and demodulation, however modulation has different meanings in literature. When discussing modulation there are three main ways in which we modulate a signal. It can be based on concentration, molecule type, and/or molecule isomers. In this report we refer to modulating based on molecular concentration, ignoring the other two categories.

1.2 Transport models

The simplest model to describe particle transport is the well-known advection-diffusion equation. We assume, for the time being, an infinite 1D domain:

$$\begin{aligned} \frac{\partial c(x,t)}{\partial t} + v\frac{\partial c(x,t)}{\partial x} - D\frac{\partial^2 c(x,t)}{\partial x^2} &= 0 \\ c(x,0) &= P(x) \end{aligned} \tag{1}$$

where c is our concentration of particles, v is the velocity of the field, D is the diffusion coefficient, and $P(x)$ is our generic initial condition.

Given a delta function as the initial condition ($P(x) = \delta(x)$), the solution localised around the arrival point (receiver) of the particles can be interpreted as a transfer function (in time). A transfer function conveniently describes how something is being transported through a medium; in this case the transfer function contains all the information needed to develop MC strategies through a homogeneous medium, and looks like the following:

$$c(x - vt, t) = \frac{1}{\sqrt{4\pi Dt}} e^{-\frac{(x-vt)^2}{4Dt}} \tag{2}$$

A more realistic model that includes possible interactions between the fluid and the porous medium is the mobile-immobile model (MIM). The porous medium itself is stationary but the model name refers to locations within the porous medium where fluid will flow as normal (mobile parts), and locations where the fluid will travel very slowly or get trapped (immobile parts). This model is essentially an advection-diffusion-reaction model problem:

$$\begin{aligned} \frac{\partial c(x,t)}{\partial t} + v\frac{\partial c(x,t)}{\partial x} - D\frac{\partial^2 c(x,t)}{\partial x^2} + \beta c(x,t) &= \beta b(x,t) + P(x,t) \\ c(x,0) &= 0 \\ \frac{\partial b(x,t)}{\partial t} &= \beta(c(x,t) - b(x,t)) \end{aligned} \tag{3}$$

where c, v, and D are the same variables and parameters as in (1), with the addition of β and b; which are the exchange rate of particles from mobile to immobile (or vice-versa) and the concentration of immobile particles, respectively. We also now have a source term $P(x)$ which can be related to the initial condition in (1) using Duhamel's principle.

This problem describes how a fluid flows in a porous medium which has both advective and diffusive properties; as well as reactivity properties relating to the exchange in particles from mobile to immobile parts of the porous medium (which is described by β and b, where b itself is represented as an ODE). It should be noted that this is a inhomogeneous PDE with a zero initial condition and a source term P, that could describe, for example, how particles are inserted in the system. The result of this problem is more complicated and has more steps to deriving an analytical solution compared to the homogeneous advection-diffusion equation.

The solutions of both these models are analysed in the appendix section of this report, were graphical representations are shown and used to analyse how the behaviour changes depending on the

parameters of the model (i.e velocity, diffusion, reactivity). However, as is common when dealing with model problems of this sort we first proceed to non-dimensionalise the whole problem. In doing so, the two problems mentioned above are transformed into the following forms:

$$\begin{aligned} \frac{\partial c}{\partial t} + \frac{\partial c}{\partial x} - \frac{1}{Pe}\frac{\partial^2 c}{\partial x^2} &= 0, \quad Advection - Diffusion - Model \\ c(x,0) &= P(x) \end{aligned} \tag{4}$$

Where c, x, t, and Pe are all dimensionless parameters; With Pe (the Peclet number) defined to be $Pe = \frac{LV}{D}$, consisting of some distance (L), speed (V), and diffusive coefficient (D). We could choose $L = 1$ and $V = 1$ for suitable simplifying purposes.

$$\begin{aligned} Pe\frac{\partial c}{\partial t} + Pe\frac{\partial c}{\partial x} - \frac{\partial^2 c}{\partial x^2} &= Da_2(b - c) + P, \quad Mobile - Immobile - Model \\ c(x,0) &= 0 \\ \frac{\partial b}{\partial t} &= Da_2(c - b) \end{aligned} \tag{5}$$

where c, x, t, Pe, and Da_2 are all dimensionless parameters with Pe still being the Peclet number and Da_2 (the Damkohler number version 2) defined to be $Da_2 = PeDa$; with Da (the Damkohler number) being defined to be $Da = \frac{\beta L}{V}$, consisting of some exchange rate (β), distance (L), and speed (V).

2 Modulation

To preface this section it should be noted that the model we study here (the advection-diffusion equation) is done so in its non-dimensional form. There are multiple different versions of the same parameters when dealing with models such as this one, like velocity: We can have a velocity at the microscopic level which would be considered to be the fluid velocity, and we can have a velocity at the macroscopic level which would be considered to be the average velocity (or Darcy velocity); these different types of velocities are important to specify as they can change the interpretation of a model and its solution. There is also the diffusive coefficient, knowing when to define it as diffusion or dispersion. In this thesis, since we are only dealing with mass transfer at the microscopic level, we will define our velocity as fluid velocity and our diffusion as a diffusive term, and not a dispersive one. One final remark is the notable absence of a porosity term which is usually found attached to the time derivative term in these equations. We omit this term for the time being only for simplicity and intend to implement it back into these models in the near future.

This chapter focuses on modulation. It explores how molecules which carry information may modulate through a porous medium and interact with a receiver, where the information will then be demodulated. The inspiration for this chapter comes from the study of information transfer and transport models, where a combination of the two areas seems to be promising in providing new ideas and results in the world of molecular communication. Taking molecules and encoding information onto them, we investigate how to retain the information we transmit through a porous medium at the receiver, with the aim to reduce the error in lost information; i.e., we aim to optimise bit error rate (BER) which is a quantitative measure describing the efficiency of a signal in the presence of noise. Firstly, we relate back to work done in the first year, extending the work done on transfer functions and applying it to a communication setting, where we modulate the information using a delta function. For illustrative and motivational purposes we provide figures showing arrival time distributions and show how symbol intervals, i.e. the times for which we wait to send a consecutive impulse, can affect the error in demodulation. We provide a mathematical framework to work from, where we discuss the simple case of a small diffusion regime. We provide analytical results in this domain. Secondly, we explore a setting where our modulating and demodulating functions are kept general, and not strictly non-negative delta impulses. We achieve a demodulating function from this generic modulating function (numerically) which will retrieve our transmitted signal and proceed to demodulate the information contained therein. This leads to the main results of the report, producing further waterfall diagrams to understand how efficient generic modulating- and demodulating- functions are in sending and retrieving a desired signal. We then play with the numerical results to observe how the results change for varying parameters and noise. We achieve these results using the mathematical tool of *singular value decomposition* (SVD).

To begin we must first discuss the mathematical framework we work from, explain what the problem is and the motivation behind studying it.

2.1 Simple Modulation

This subsection provides the motivation and qualitative illustrations for the ideas proposed in this report, including an extension on the research carried out during my starting period, with figures of arrival time distributions of the advection-diffusion equation discussed. We discuss the mathematical framework from which we work from and briefly look into symbol interval optimisation, to show how this simple process becomes intricate when one tries to optimise the problem of information transfer. When we are able to send information as quickly as possible with as low an error rate as possible then we have achieved our optimisation, and we have therefore optimised the problem – this optimisation process is discussed in more detail throughout the report, but put simply we are trying to model the most efficient communication method (optimal approach) by improving on ideas used in literature using novel ideas (optimising work done). This whole process would have the end goal of completely improving on previous work done in the field, finding the best way of communicating through a porous medium (optimisation of the problem) – optimal, optimising, and optimisation are just terms used in this report to address the improvements to be made in communicating within a porous medium, relating to fast information transfer with low error rates. Firstly we look at what the problem is and how we think about the optimisation of the information transfer problem, Secondly we create the mathematical/communication framework from which we work from when studying these problems, and lastly we discuss how optimising this simple process becomes difficult when considering the practicalities of the problem; such as the need for multiple impulses/symbols in a constrained time frame. We therefore discuss what the problem is, what this thesis focuses on optimising, and how we tackle this optimisation problem. Some quantitative results are also produced in relation to work done in section (2.2.3).

For a given channel we can calculate its corresponding transfer function, which in-turn will describe how particles in the channel travel throughout it. For purposes of testing our approach, we begin with a simple advection-diffusion channel (4.1.1) and take its transfer function convoluted with a delta impulse, which yields the following figure:

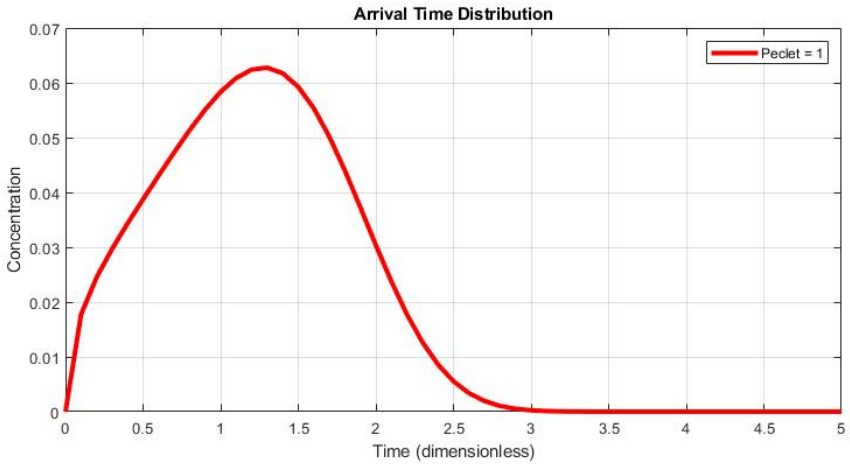

Figure 3: Arrival time distribution for particles reaching the receiver under the advection-diffusion model.

where this curve represents the information (bits), x_i, we send in one impulse/symbol through the porous medium; impulse/symbol refers to the transmission of an individual block of information of length m, and is dependant on the transfer function. This information is encoded into the concentration of the molecules we impulse into the porous medium. This idea is explored in further detail in [46], with an isomer-based concentration shift keying (ICSK) approach taken for the transfer of information. For our purposes, the idea of using concentration to transmit information remains the unchanged, and is described in our simplified models by the delta function impulsing the molecules into our system. Fig. 3 is known as the *arrival time distribution*, and gives the probability density of a particle reaching the receiver at a given time. Note that this means the integral of this transfer function across all time is equal to 1. Practically, however, when receiving the transmitted signal one does not usually have enough time to wait to receive the entire symbol before sending/receiving a consecutive symbol. If we limit ourselves to having, say, 1 minute to send and receive information, then we have a restriction on how many symbols we can physically transmit during this time. This means that the curve is potentially overlapped with another curve at some time instant, τ, due to a consecutive symbol being transmitted, resulting in the study of inter-symbol interference. I.e., a consecutive transmitted symbol interferes with the first symbol sent. Studies such as [47] attempt to optimise this process which depends on multiple factors, such as symbol intervals (length of τ), Peclet values, etc.

The problem we are investigating is how to optimise a generalised version of this problem. Namely, we look at a general modulation where we no longer have delta impulses (symbols) in particular carrying our information. The benefit of using a general modulation rather than a delta function is that we are no longer restricted by how many symbols we can send. We aim to no longer restrict ourselves to symbols being activated at certain times, but instead have a continuous stream of information being transmitted. The limitation of this problem is that it is more difficult to solve analytically, resulting in the need for numerical approaches; where we begin working from our mathematical framework. However, before moving to the general setting we first discuss simplest case of this optimisation problem and the practical issues in sending information. This gives rise to a second motivation for the research in this report. We briefly look at what happens when we have a delta function as our channel model. We then conclude this section with an illustration showing the complexity of the problem when we want to send multiple symbols consecutively after each other.

Before studying the simple case we must first define the mathematical/communication framework from which we will be working from.

2.1.1 Communication framework

We have a continuous signal in time we wish to send across a channel, denoted by $x(t)$. $x(t)$ is known as the input signal and is a continuous function of $t \in \mathbb{R}$. This input signal is composed of a family of functions, $\phi_i = \Phi$, which exists in the continuous function space $C^0([0,T])$ over some time interval T, and the bits we are transmitting, x_i, which is a string of digits of length b for each bit $i = 1, 2, ..., N$. We therefore have the following formula for composing a signal in general:

$$x(t) = \sum_{i=1}^{N} x_i \cdot \phi_i(t) \tag{6}$$

where x_i is considered to be the information sent ($0's$ and $1's$) and ϕ_i are the modulating functions. In general they are not just multiplied together, but undergo the dot product and are defined as $x_i \in \{0,1\}^b$ and $\phi_i = (\phi_{i1}, ..., \phi_{i,b})^T$; where b is the (block) length of bits sent and ϕ is some column vector of equal length. If $b = 1$ then this dot product becomes a multiplication. There is a constraint placed on the modulating functions ϕ_i which is dependent on the concentration of the particles being sent; it is not physical to have $|\phi_i| < |\phi_i \cdot X_i|$ as this would mean we want to send more information than our modulating function can process.

We aim to retrieve the input signal, x_i, completely, obtaining the desired signal, y_i. That is we want to obtain $y_i \in \{0,1\}^b$ such that $|y_i - x_i| = 0$. However, obtaining the exact bits of information sent is not likely, and errors will often be present due to noise in the channel, or other external factors. Adjusting for this we instead require $y_i \in \{0,1\}^b$ such that $|y_i - x_i|_1 < \epsilon$, where ϵ is a small number quantifying a threshold error and $|\cdot|_1$ is the L1 norm. To obtain y_i we must first process what we call the output signal, denoted by $y(t)$, which is the convolution in time between the input signal and some function, $h(t)$, describing the channel we pass our information through. This is commonly referred to as the transfer function of the channel.

$$y(t) = x(t) * h(t; K) = \int_0^t x(t-\tau) h(\tau; K)\, d\tau \tag{7}$$

$h(t)$ is a function continuous in time and varies with changing parameters, $K = (\kappa_1, \kappa_2, ..., \kappa_n)$, having '$n$' many parameters. Note the operation $'*'$ represents the convolution operation in time. However, if we move into frequency space this operation becomes a product. In order to preserve the generality of this description we will refer to $'*'$ as the '*star*' operation. We then multiply this output signal against the function, $\tilde{\phi}$, which also exists in the continuous function space $C^0([0,T])$ over some time interval T. $\tilde{\phi}$ is what we call the demodulating function.

Applying this problem to a transport model, we can study what happens when we take the known transfer function associated with the advection-diffusion equation, $h(t)$. In this case we have the following operation to retrieve the transmitted signal:

$$y_j = \sum_{i=1}^{N} x_i \int_0^{\infty} \left(\phi_i(t) * h(t; x_R, Pe)\right) \tilde{\phi}_j(t)\, dt \tag{8}$$

where x_R is the location in space of our receiver, and $Pe = \frac{LV}{D}$ is the Peclet number. Note that for simplicity we now choose the block length of our bits to be $b = 1$

That is, to retrieve the desired input signal consisting of the bit x_j, we can equate the following relationship:

$$y_j = \sum_{k=1}^{N} x_k \int_0^{\infty} \left(\phi_k(t) * h(t; x_R, Pe)\right) \tilde{\phi}_j(t)\, dt = x_j + O(\epsilon) \tag{9}$$

where $O(\epsilon)$ accounts for some error in the information transfer process. Specifically, $O(\epsilon)$ is the quantitative difference between the information we input into the system and the information which is output from the system.

The mathematical complexity of this problem is contained in the double integral (hidden implicitly by the convolution operator), the rest of the terms are simple inputs which are known. Therefore we can say that to observe a signal at the receiver we must require this double integral to equate to 1, or 0 if no signal is observed. This is due to the fact the double integral contains all the information of the transfer process. For this transfer to be observed the concentration of the particles being transferred must be measured, which is done so by calculating the double integral, yielding the concentration of particles at the receiver; thus giving the concentration of the signal being sent reaching the receiver, where we normalise the integral. So our focus in the communication framework is to understand and optimise the following identity:

$$\int_0^\infty \int_0^t \left(\phi_i(t-\tau)h(\tau; x_R, Pe)\right)\, d\tau\, \tilde{\phi}_j(t)\, dt = \delta_{ij} + O(\epsilon) \tag{10}$$

where δ_{ij} is the Kronecker delta. $O(\epsilon)$ appears again on the right side of this equation due to the fact we are using the modulating and demodulating functions which we choose to be bi-orthogonal. However, the operation between these two functions is not exactly the scalar product, which would be equal to 1. So in this sense we take the operation to be as close to 1 as possible as this resembles the orthogonality between the two functions.

From this identity we obtain the following theorem:

Theorem 1. *Let $\phi_i(t) = \Phi$ and $\tilde{\phi}_j(t) = \tilde{\Phi}$ be two exclusive sets of continuous functions, and let $h(t; K(\kappa))$ be a continuous function in time, varying with parameters $K = (\kappa_1, \kappa_2, ..., \kappa_n)$. If*

$$\int_0^\infty \int_0^t \left(\phi_i(t-\tau)h(\tau; K)\right)\, d\tau\, \tilde{\phi}_j(t)\, dt = \delta_{ij} + O(\epsilon) \tag{11}$$

then we have

$$|y_i - x_i| = O(\epsilon) \tag{12}$$

for some input x_i and output y_i.

which is proved in the appendix, section (4.2.1)

If we can optimise this double integral, i.e. be as close to 1 as possible, thereby reducing this error difference $O(\epsilon)$, then we have created an efficient communication process. Schematically the process looks as follows:

$$\mathrm{x} \in \{0,1\}^b \xrightarrow{\textbf{modulate}} \mathrm{X(t)} = \sum_i^N x_i\phi_i(t) \xrightarrow{\textbf{Transmit}} \mathrm{Y(t)} = \mathrm{X(t)*h(t)} \xrightarrow{\textbf{Demodulate}} y_j = \mathcal{D}\left(Y(t)\right) = \int_0^{t'} Y(t)\tilde{\phi}_j(t)\, dt$$

where we recall b represents the length of the bit, and $\mathcal{D}$ defines the generic demodulating operation.

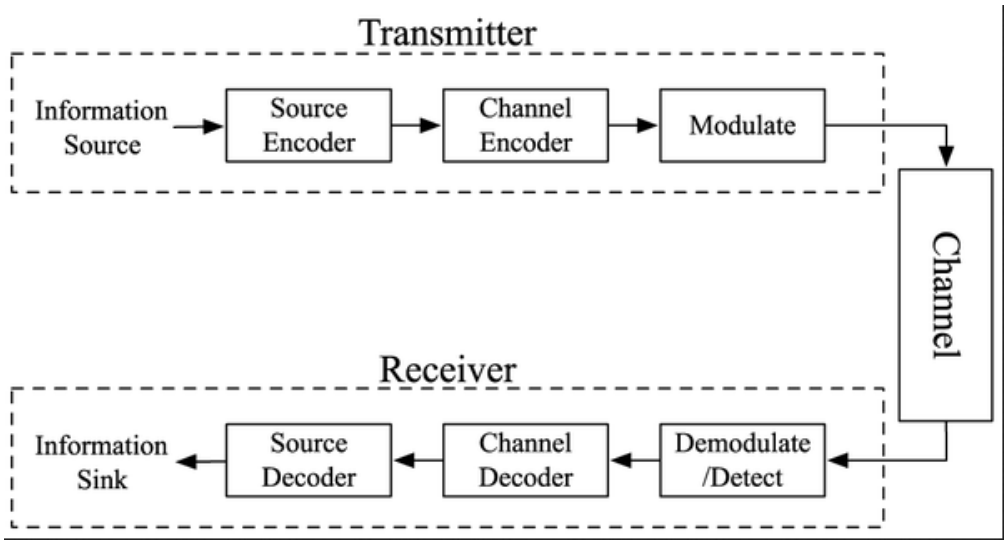

Figure 4: A block representation of the modulation-demodulation process we look at in this report ([48], Materials and Methods)

2.1.2 Channel model: Delta function

This section deals with simple modulation, both in the mathematical sense and physical sense in order to get some intuition of the behaviour of the problem; with the equations being studied becoming simpler (ϕ_i no longer needs to be continuous) and the physical process being trivial and unrealistic. Throughout this section we deal with

$$\phi_i = \delta(t - T_i)$$

which represents an impulse of information being injected into our system at some time $t = T_i$. We consider a system where the channel $h(t) = \delta(t)$ is also modelled by a delta function, known as a *small diffusion regime*.

For $\phi_i(t) = \delta(t - T_i)$ recall the following definition:

$$\begin{aligned} y_j &= \int_o^T \big(X(t) * h(t)\big)\, \tilde{\phi}_j(t)\, dt \\ &= \int_o^T \left(\sum_{i=1}^N x_i \delta(t - T_i) * h(t)\right) \tilde{\phi}_j(t)\, dt \\ &= \sum_{i=1}^N x_i \int_0^T \int_o^t \delta(\tau - T_i) h(t - \tau)\, d\tau \tilde{\phi}_j(t)\, dt \\ &= \sum_{i=1}^N x_i \int_0^T h(t - T_i) \tilde{\phi}_j(t)\, dt \end{aligned} \tag{13}$$

Eq. 13 is our starting point when in this simple modulation case.

From here we move to the small diffusion regime by taking $h(t) = \delta(t)$, which yields the following:

$$\begin{aligned} y_j &= \sum_{i=1}^{N} x_i \int_0^T \delta(t - T_i)\tilde{\phi}_j(t)\, dt \\ &= \sum_{i=1}^{N} x_i \tilde{\phi}_j(T_i) \end{aligned} \tag{14}$$

So for a delta impulse as our modulator, and a delta function as our transfer function, our received information is proportional to the demodulating function. We can infer that if we desire the output information to be the same as the input information (i.e. $y_q = x_q$, no error) then we have the following equation:

$$\begin{aligned} x_j &= y_j \\ &= \sum_{i=1}^{N} x_i \tilde{\phi}_j(T_i) \end{aligned} \tag{15}$$

From the property of the Kronecker delta function we obtain the following condition for our demodulating function:

$$\tilde{\phi}_j(T_i) = \delta ij \tag{16}$$

So in the small diffusion regime we look to find functions which satisfy condition (16), such as the rectangular wave-front function defined as:

$$\tilde{\phi}_j(t) = \Theta(t - (T_j - \frac{\Delta t}{2})) - \Theta(t - (T_j + \frac{\Delta t}{2})) \tag{17}$$

where Θ is the *Heaviside function* and Δt is it's width.

That is to say, if we have a delta function (as our transfer function) within the compactly supported rectangular function then we have perfect demodulation. However, a delta function is not a realistic transfer function, and more realistic transfer functions should be studied.

Another simple modulation case, this time with an oscillatory channel, is discussed in the appendix section (4.2.5) of this report; with work still needing to be done on it.

2.1.3 Channel model: ADE

Note that the limiting case of the advection-diffusion transfer function (diffusion $\to 0$) becomes a small diffusion regime problem. Thus the advection-diffusion equation is the logical step to move to more realistic transfer functions. More realistic transfer functions are harder to demodulate information from as they have more dispersive features. These dispersive features, in particular the "fat tails" produced by them, are what cause problems when demodulating information

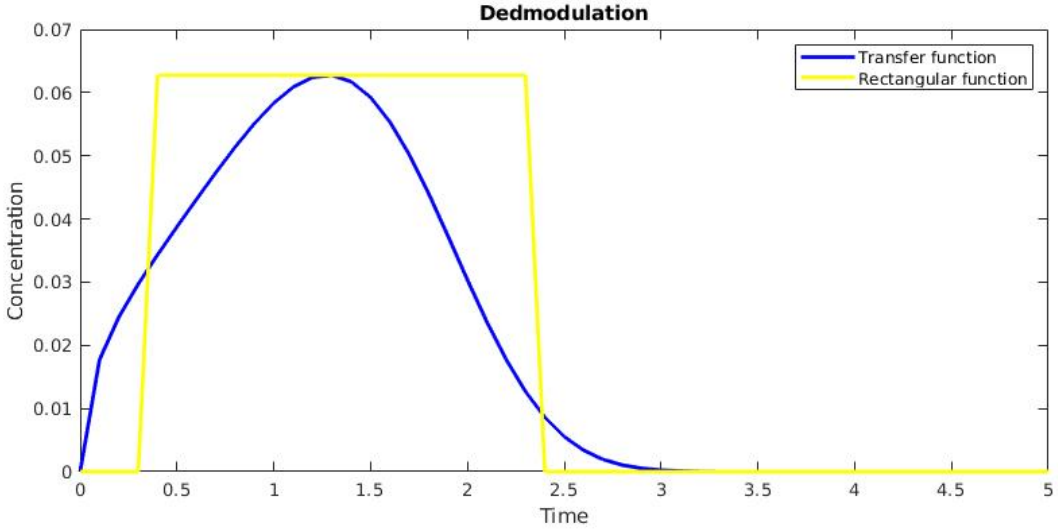

Figure 5: An illustration of demodulating an impulse/symbol. The Heaviside function and transfer function coincide with one another over some time interval Δt. This overlap between the two functions corresponds to the symbol being demodulated at the receiver and the information being retrieved. Note that only the area of the transfer function under the Heaviside function is demodulated, as the rest becomes zero. This relates to the receiver only being activated for the time interval during which the Heaviside function is 'activated'.

across a medium. If we take a look at Fig. 5 we observe a rectangular function (in yellow) and the advection-diffsuion transfer function (in blue). We can observe that not all of the transfer function is contained within the rectangular function. This relates to information being lost in the medium. This feature is common in more realistic transport models, and the problem is not easily fixed. For instance, we can not simply extend the width of our rectangular function to be arbitrarily wide and contain all the information of the transfer function inside it. This is because there are practical problems to consider. One such problem is that multiple signals tend to be sent together, meaning there will be a consecutive signal, similar to the transfer function shown in Fig. 5 (blue), sent shortly after the first one. This means the rectangular function (if arbitrarily wide) may take information from the consecutive signal also, which causes interference. This is what is known as inter-symbol interference and is part of the problem of having an arbitrarily wide rectangular function as our demodulating function. This extension to having multiple symbols is the second motivation of this report. We would like to not be restricted by how many symbols we can transmit in a given time frame. Illustrations are given next to motivate the reason why we move into a generic modulation setting, instead of staying in a delta modulation setting.

We now move away from the small diffusion regime and look at channels which are more realistic, coming from transport models. Particularly, we are now looking at the advection-diffusion transfer function, under the influence of a delta impulse as our modulating function. Theoretically one could wait a large amount of time to obtain an entire signal sent by the transmitter before sending another signal, but doing this is not practical. The practical way to send and retrieve infor-

mation is to wait a much shorter amount of time with a concentration threshold. This threshold, if met, decides if the signal being sent has been retrieved. To retrieve the information a demodulating function would be needed to recover the signal, and for this specific case the demodulating function would be the Heaviside function, shifting through time along with the transmitted symbols; note that the Heaviside function would only need to be activated during a time interval around when a delta function was activated. The end of the Heaviside time interval corresponds to when the transmitted signal stops being retrieved.

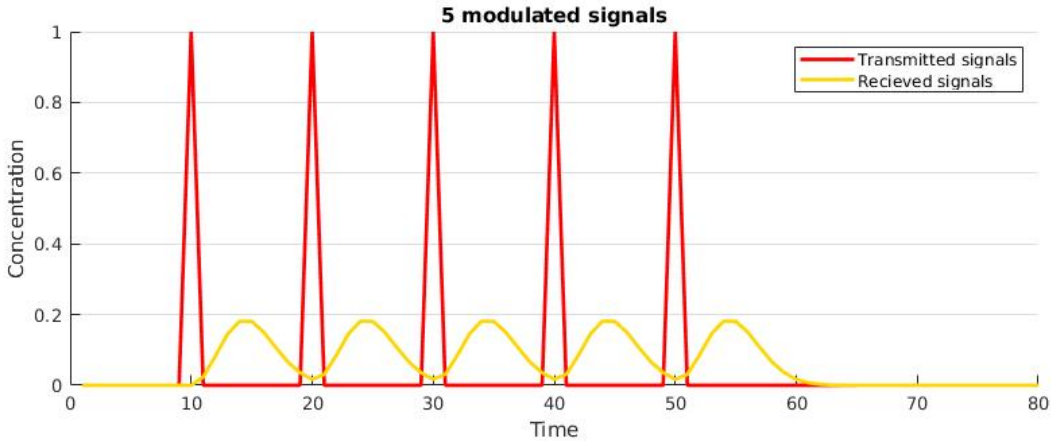

Figure 6: An illustration of modulating 5 impulse symbols into a medium, with a temporal delay waiting until each signal reaches the receiver before sending a consecutive signal.

Fig. 6 depicts neatly the overall process from modulation to demodulation, previously discussed from a mathematical perspective. This plot represents 'sufficiently spread' modulations, resulting in inverse Gaussian fluctuations at the receiver, which is coinciding with what the mathematics describes. The term 'sufficiently spread' is used here when referring to the time spent between sending consecutive symbols being long enough for most of the previous signal to reach the receiver.

We now ask the question, "*what would happen to the symbols when we observe 'inconsiderate' spreading of symbols*"? By 'inconsiderate' we mean a consecutive signal would be sent before most of the prior signal has reached the receiver. This report does not venture further into this problem from a quantitative stand point. However, the concept is relevant to the problem we do investigate and so taking time to discuss this problem qualitatively is beneficial in understanding the motivation behind the problem studied in this report. Returning to our transfer function we obtain the following graphical illustrations of this process:

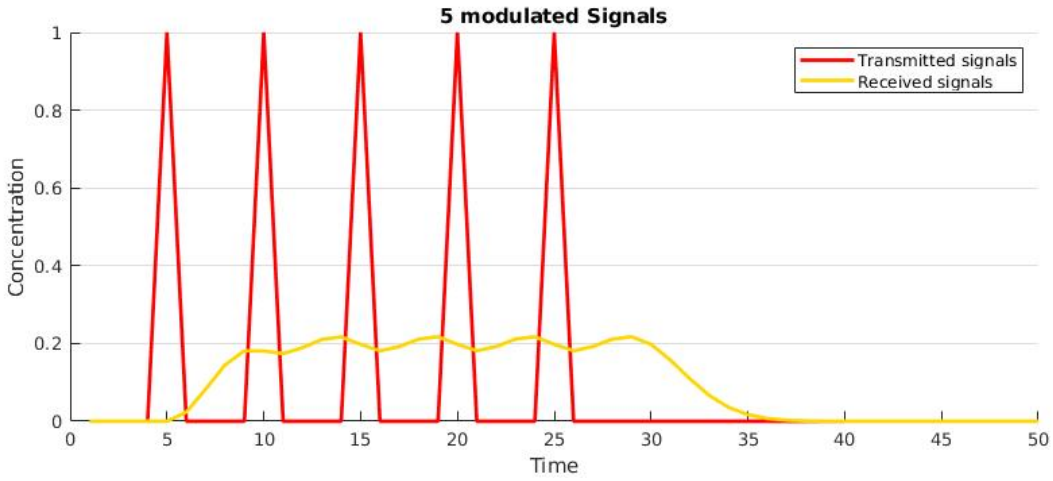

Figure 7: An illustration of modulating 5 impulse symbols into a medium, with an inconsiderate temporal delay between sending each impulse. This results in the symbol not being able to fully reach the receiver before a consecutive symbol is sent.

Observing Fig. 7 we notice that the received signal (all the individual symbols), depicted by the gold curve, loses its oscillating inverse Gaussian structure compared to Fig 6. This is due to the time between sending each symbol being halved, resulting in the receiver not being able to demodulate most of the previous symbol before the consecutive symbol reaches the receiver. This leads to larger errors in the demodulation process since we cannot obtain the full signal sent via its individual symbols before they are corrupted with a second, third, or fourth, etc, symbol. This means to obtain the probability of receiving the desired signal, we need to integrate the received symbol of each impulse separately and cannot combine the symbols together.

Since symbols can become convoluted with each another, making them less desirable, one way to improve the efficiency of receiving the desired signal is to optimise the delay between sending consecutive symbols. A proposal of delaying certain signals throughout the transmission process in order to optimise the error rate of our signal may be beneficial [47]; this paper looks at the optimisation of time spent between sending signals, and how a small delay in certain intervals of time can increase the efficiency of detecting a desired signal.

Fig 8 gives a graphical illustration of the switching on and off of 10 symbols, where we switch off symbol 3 and symbol 8. A pattern emerges in the concentration of the received signal giving some qualitative insight into how symbol interval optimisation can be of importance in retrieving a desired signal.

Now, if we take this idea of modulating multiple symbols in a constrained time frame to create a desired signal and extend it, we arrive at our problem. We take these ideas further by moving into a more general setting, investigating how to optimise information transfer of a signal which can not be broken up into different delta impulses, but is instead one continuous stream. I.e. we do not choose what our modulating function looks like nor control time intervals at which to acti-

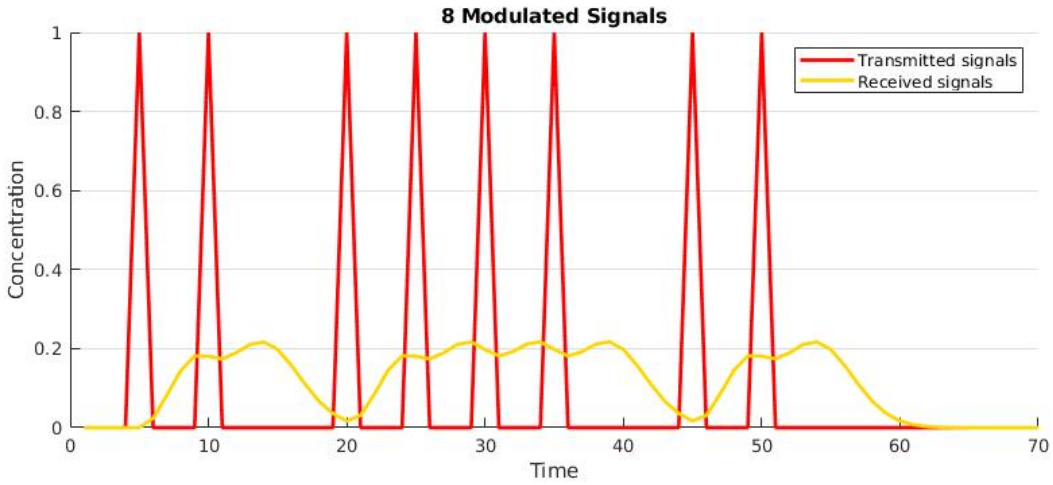

Figure 8: An illustration of modulating 8 impulse signals into a medium, with 2 signals being switched off. It is clear that the temporal delay between impulses effects the received signal.

vate individual symbols, omitting of course the first time we activate the signal. This idea makes use of biorthogonal functions and is the novelty of this report.

2.2 Generic Modulation

When having a generic transfer function, and applying the mathematical framework described in section (2.1.1), recall the demodulation process from a mathematical perspective is written as follows:

$$y_j = \int_0^\infty Y(t)\tilde{\phi}_j(t)\,dt = \int_0^\infty \left(\sum_{i=1}^{N} x_i \phi_i(t) * h(x_R, t) \right) \tilde{\phi}_j(t)\,dt \tag{18}$$

where $\phi_i(t)$ is the generic modulating function, x_i is the bits (information), $h(x_R, t)$ is the transfer function, and $\tilde{\phi}_j$ is the demodulating function. The quantity of interest is this convolution integral:

$$\int_0^\infty \int_0^t \left(\phi_i(t-\tau)h(x_R,\tau)\right)\, d\tau\, \tilde{\phi}_j(t)\,dt = \delta_{ij} + O(\epsilon) \tag{19}$$

and as explained in section (2.1.1), if we can optimise this operation we have optimised the information transfer problem in a generic setting.

Solving this equation analytically in order to obtain a solution between the ouput and input is difficult due to the presence of the convolution operation, thus it is more convenient to arrive at a set of modulating and demodulating functions, which can retrieve the signal, from a numerical approach. We therefore move from the continuous setting to a time-discretised setting. The reason for doing so is to use singular value decomposition (SVD) to obtain a bi-orthogonal system

of modulating functions and demodulating functions directly. However, the continuous approach is investigated further in section (4.2.3), with a brief discussion on a similar problem. A solution to this problem is found in Fourier space, inferring an analytical solution to this generalised problem may be possible to find; this is future work to be looked into at a later date. It should also be noted that a further approach was taken, deriving a procedure to obtain a set of modulating and demodulating functions (discussed in appendix, 4.2.2).

2.2.1 Modulation-Demodulation scheme in discrete time

The entire process from modulation to demodulation of a signal is schematically shown below. This is where we introduce the novel idea of using biorthogonal functions, denoted as our modulating and demodulating functions respectively.

$$\mathbf{x} \in \{0,1\}^m \xrightarrow{\textbf{modulate}} \mathbf{X}_{1\times T} = \mathbf{x}_{1\times m}\mathbf{\Phi}_{m\times T} \xrightarrow{\textbf{Transmit}} \mathbf{Y}_{1\times T} = (\mathbf{X}_{1\times T} + \eta_M)\mathbf{H}_{T\times T} + \eta_A$$
$$\xrightarrow{\textbf{Demodulate}} \mathbf{y}_{1\times m} = \mathcal{D}(\mathbf{Y}) = \mathbf{Y}_{1\times T}\bar{\Phi}_{T\times m}$$

where m is the number of modes, T is the length of our discrete time, $x \in \mathbb{R}^m$ is the information that is encoded and modulated, $\mathbf{X} \in \mathbb{R}^T$ is our transmitted signal, $\mathbf{\Phi} \in \mathbb{R}^{mxT}$ is our carrier matrix, $\mathbf{H} \in \mathbb{R}^{TxT}$ is our transfer matrix obtained by using a *Toeplitz matrix*, $\bar{\mathbf{\Phi}} \in \mathbb{R}^{Txm}$ is our demodulating matrix, $\mathbf{Y} \in \mathbb{R}^T$ is the reception of the transmitted signal, $y \in \mathbb{R}^m$ is the obtained signal, and η is the noise of the system; with η_M denoting the multiplicative noise and η_A denoting the additive noise. The location of η represents what type of noise it is (additive or multiplicative); if located within the product of the transmitted signal and the transfer function it is called a '*multiplicative*' noise, whereas if it is just added to the product it is called an 'additive' noise. Although not shown here, it is important to mention that each type of noise results in different values for the error of the demodulation process.

Working off this schematic, we propose a mathematical framework to approach this problem from. This mathematical framework can be condensed down from Theorem 1, which is clearly considered in continuous time, so its discrete analogue can simply be written as:

Theorem 2. *Let* $\mathbf{\Phi}$ *and* $\bar{\mathbf{\Phi}}$ *be two exclusive sets of matrices, and let* $\mathbf{H}$ *be a discretised matrix in time. If*

$$\mathbf{\Phi}\mathbf{H}\bar{\mathbf{\Phi}} = \mathbf{I} + O(\epsilon) \tag{20}$$

then we have

$$|\mathbf{y} - \mathbf{x}| = O(\epsilon) \tag{21}$$

for some input $\mathbf{x}$*, output* $\mathbf{y}$*, and identity matrix* I*.*

In this proposition, we assume for simplicity that we know the entries of the transfer matrix $\mathbf{H}$. The entries for matrix ϕ are defined to be $\mathbf{\Phi}_{ik} = \phi_i(t_k)$, and is as such similar for the entries of the other matrices. If we are able to retrieve the modulating and demodulating matrices such that Eq. 20 holds then we have successfully found a modulating-demodulating process which works.

Skipping over further details we now introduce the singular value decomposition (SVD) method.

2.2.2 Singular Value Decomposition of The Transfer Function

Remaining in a discrete setting, we move towards observing the attenuation behaviour of our system. Attenuation refers to a reduction in signal strength and thus is directly related to the transmission of such signal; this is also known as *'path loss'* in power based calculations of canonical communication systems based on electrical signals. Attenuation can be calculated from the transfer function of the system (or better yet the reception of the signal) and thus we analyse the transfer function.

In this report, which leads to aim towards the fundamental idea of 'bridging the gap' between fluid mechanics and information theory, we will interchange our transfer function H (also referred to as the 'channel'), derived from a transport model, with the attenuation of the system.

Singular value decomposition (SVD) is a method used in this report as it speeds up the optimization process. Put simply, it reduces a matrix to its constituent parts to make matrix calculations simpler. It achieves this by factorising a real, or complex, pxq matrix into three other matrices in the form of $U\Sigma V^T$; where U is a pxp unitary matrix, Σ is a pxq diagonal matrix, and V is a qxq unitary matrix. This report makes use of the incomplete SVD, which differs from the complete SVD as it only takes the essential information from the matrix needed to compute the problem; i.e., we take an approximation of $H \approx U\Sigma V^T$, which is a truncated version of the SVD, rather than the complete form of $H = U\Sigma V^T$. This is explained in further detail in the appendix section. The essential information relates to the number of bits (m) being sent, which means we only consider m modes of the matrix and no more. Taking (20) we can expand H in its SVD form as follows:

$$\Phi U\Sigma V^T\tilde{\Phi} = I \tag{22}$$

where U and V are orthogonal matrices, with Σ being a diagonal matrix.

Note that if we had kept the error term $O(\epsilon)$ in Eq. 20 then we could have written it as

$$\Phi H\bar{\Phi} \approx I \tag{23}$$

which in turn would mean Eq. 22 would look like

$$\Phi U\Sigma V^T\tilde{\Phi} \approx I \tag{24}$$

which is the incomplete SVD formalism (since $H \approx U\Sigma V^T$ in the incomplete version). That is to say that the error term is present in the incomplete SVD, but for simplicity we omit the error term when discussing the ideas of SVD.

The benefit of expanding H in its SVD form is that it allows for us to write both our modulating and demodulating matrices in terms of the orthogonal matrices U and V respectively. To show this we can write H explicitly as such:

$$H = U\Sigma V^T \tag{25}$$

Taking $H^T H$ and HH^T separately yields:

$$\begin{aligned} H^T H &= (V\Sigma^T U^T)U\Sigma V^T = V\Sigma^T \Sigma V^T \\ HH^T &= U\Sigma V^T (V\Sigma^T U^T) = U\Sigma\Sigma^T U^T \end{aligned} \tag{26}$$

This suggests that the orthogonal matrices U and V are simply the eigenvectors of HH^T and $H^T H$ respectively, and $\Sigma^T\Sigma$ (or $\Sigma\Sigma^T$ since diagonal) is the eigenvalue matrix of $H^T H$ or HH^T. If possible to find these eigenvectors, a relationship is needed to see how to make use of U and V for Φ and $\tilde{\Phi}$. Looking at (22) we see a solution to this equation is to write the modulating and demodulating matrices as follows:

$$\begin{aligned} \Phi &= \Sigma^{-1} U^T \\ \tilde{\Phi} &= V \end{aligned} \tag{27}$$

where the matrix Σ is obtained by taking the roots of the eigenvalues of the matrix $\Sigma^T\Sigma$ (or $\Sigma\Sigma^T$). Substituting 27 directly into 22 is performed below, showing it is indeed a suitable solution:

$$\Phi U\Sigma V^T \tilde{\Phi} = \Sigma^{-1} U^T U\Sigma V^T V = \Sigma^{-1}\Sigma = I \tag{28}$$

2.2.3 Optimising signal error

The benefits of using SVD of the transfer function is that it yields an optimal set of modulating and demodulating functions. However, the set of functions that the SVD yields may not be practically viable. It may be that the functions are difficult to work with, and so an engineer trying to produce these set of functions, which could be highly oscillatory, may struggle. Therefore, one option could be using the incomplete SVD to reduce the number of optimal solutions, yielding just one in the case of the so called 'thin SVD'. The thin SVD takes only the diagonal values of the matrix, giving benefits such as speed of calculation and economically more efficient. This would give a set of optimal solutions based on the eigenvalues of the eigenvectors used in the SVD. However, the problem still arises in the practical setting if these functions are not easy to handle; for this reason approximations are made of an SVD of the transfer function in this report, with the idea of approximating a complex function with multiple simpler functions.

To choose the modulating and demodulating functions we begin by choosing the type of modulation we want to achieve, which is driven by a stream of $0's$ and $1's$. We combine this information along to the modulating function Φ. This generates a signal with which we can calculate how the information is transported by multiplying the transfer function with the signal itself, denoted Y. To yield the signal sent we multiply Y by the demodulating function Ψ.

What should be expected in the modulation-demodulation scheme is a delay from when the signal gets modulated to when it gets demodulated. This delay is one example of how errors can occur within signals. If the delay between modulation and demodulation is long, then knowing for certainty if the signal we are demodulating is being demodulated at the correct time is not possible. Thus, approximations are made, with bit error rates (BER) calculated to estimate how many errors are sent per signal.

If we take the advection-diffusion equation for different values of the Peclet number we obtain the following arrival time distributions

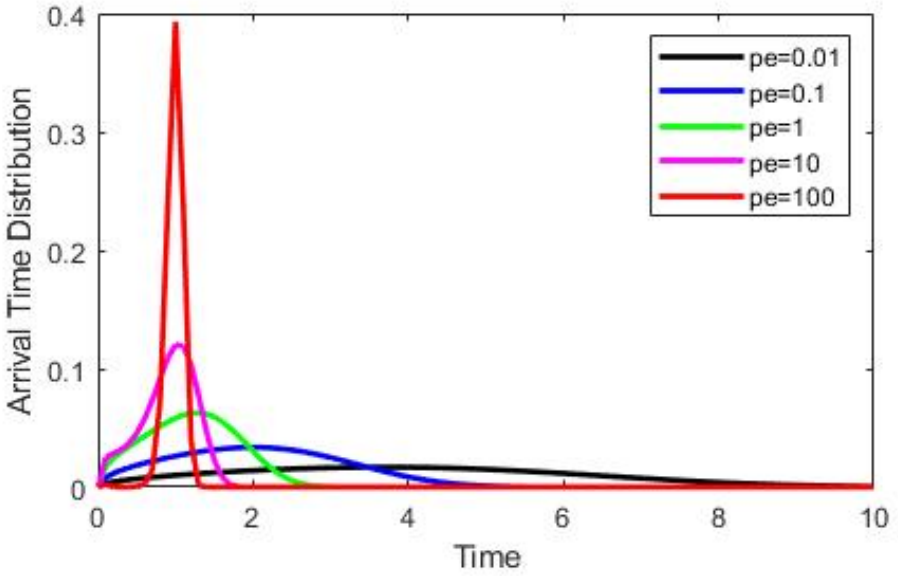

Figure 9: Arrival time distributions for varying Peclet values. As the Peclet value reduces the distribution of the curves become more dispersed, which is representative of high diffusivity within the channel.

Taking these transfer functions we can plot the waterfall diagrams of each one, resulting in a quantitative measurement of how efficient these transfer functions are in transferring information in the presence of noise.

The two types of noise we consider are multiplicative noise and additive noise. The former represents a system where the information being transmitted is affected by some disturbance in the transmission process. Mathematically, that is to say that we add a noise term, η_M, within the product of the transmitted signal $\mathbf{X}$ and the Toeplitz transfer matrix $\mathbf{H}$, as depicted in the schematic in section (2.2.1). The latter is a system where the information being transmitted is affected during the reception of the information being sent. Mathematically, we again add a noise term, η_A, but this time located outside of the product between the transmitted signal and transfer matrix.

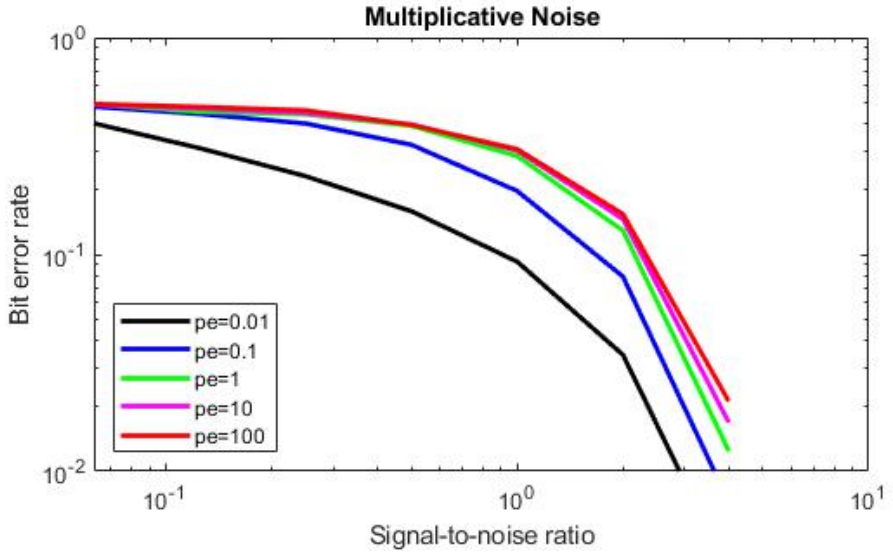

Figure 10: The signal-to-noise ratio vs bit error rate trajectory (known as waterfall diagrams due to their shape) is shown for varying Peclet values in the presence of multiplicative noise, η_M. The waterfall diagrams illustrate the error rate of information transfer in the presence of noise. For the smaller Peclet values, i.e., the more dispersive channels we notice that the error in receiving a signal is reduced compared to more velocity driven channels.

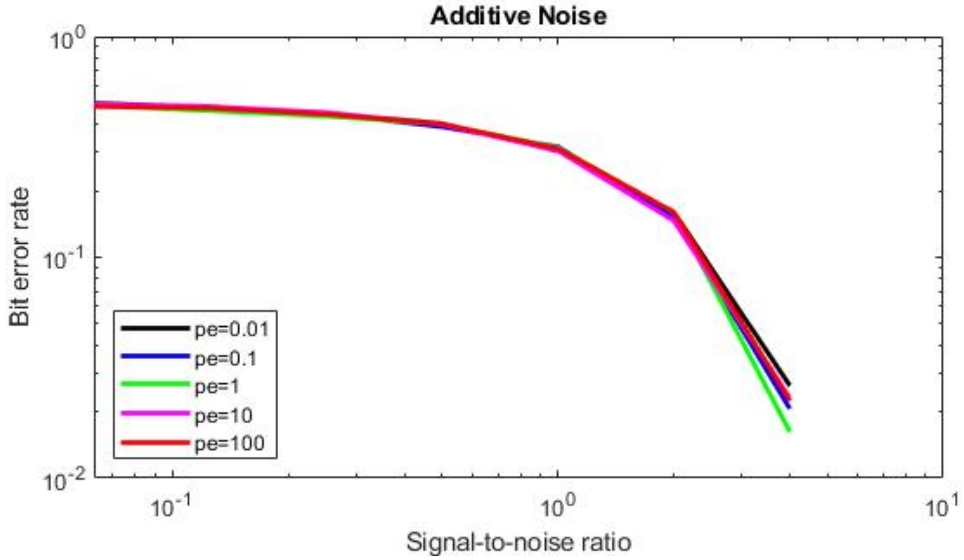

Figure 11: The signal-to-noise ratio vs bit error rate trajectory is shown for varying Peclet values in the presence of additive noise, η_A. For the smaller Peclet values, i.e., the more dispersive channels we notice that the error in receiving a signal is reduced compared to more velocity driven channels.

These results corroborate the work being done in literature [47]. In literature, waterfall diagrams

tend to plot the bit error rate of a process vs. the signal-to-noise ratio of the process. recall bit error rate (BER) is the quantitative measure of how efficient a process is in obtaining bits of information, and signal-to-noise ratio (SNR) is the quantitative measure of how strong noise is within a system. What these waterfall diagrams show is that each transfer functions decrease in error as the signal to noise ratio increases (noise decreases). Fig. 10 shows that as the signal strength increases the error in modulation of the signal decreases when in the presence of multiplicative noise. With Fig. 11 showing this effect is less diverse whether you are in a diffusive or advective driven channel, which is counter-intuitive. This effect is likely driven by the different nature of the two noise terms. Although they both affect the transmitted signal, they affect it in different ways due to the location of where the noise occurs. Clearly, having noise in the transmission process is more noticeable, due to the differing BER curves, compared to having noise in the reception process.

This approach, however, is different from approaches used in literature, with the novelty coming from the use of bi-orthogonal functions. This novelty enables one to optimise modulation through manipulation of the channel/transfer function, rather than molecule manipulation at the transmitter/receiver, or estimating the channel using numerical simulations.

3 Conclusion

There are three main points to conclude this report. They relate to the use of the mathematical framework, the use of SVD, and the presence and location of noise in the system.

1. To find an optimal set of modulating and demodulating functions, singular value decomposition provides a framework to begin working from. SVD yields one pair of optimal solutions rather than a whole set. This means that we do have an optimal solution for the modulation/demodulation scheme, however its limitation is that the optimal solution it yields may not be practically feasible to work with; for instance it may be highly oscillatory. This leads to the potential need to approximate the modulating function, resulting in extra errors. These errors can be quantified numerically, resulting in BER's and relationships between the error density and noise.

2. The mathematical framework provides a rigid starting point when dealing with optimisations of communication across a channel. In particular, the theorem:

   Let $\phi_i(t) = \Phi$ and $\tilde{\phi}_j(t) = \tilde{\Phi}$ be two exclusive sets of continuous functions, and let $h(t; K(\kappa))$ be a continuous function in time, varying with parameters $K = (\kappa_1, \kappa_2, ..., \kappa_n)$. If

   $$\int_0^\infty \int_0^t \left(\phi_i(t-\tau)h(\tau;K)\right)\, d\tau\, \tilde{\phi}_j(t)\, dt = \delta_{ij} + O(\epsilon) \tag{29}$$

   then we have

   $$|y_i - x_i| = O(\epsilon) \tag{30}$$

   for some input x_i and output y_i.

   is the key result to take away from the mathematical framework.

3. The introduction of noise has an affect on how efficiently information is passed through a channel. In particular, the location of the noise term plays an important role. If it appears in the product between the signal and transfer function (multiplicative noise) then the diffusivity of the channel plays a more prominent role. However, if the noise is outside of the product (additive noise) then the diffusivity of the channel appears to be not as important. That is to say the BER does not change regardless of how diffusive the channel is.

In conclusion, when modulating a signal through a porous medium we have a start point given by the mathematical framework. It is beneficial to use the SVD method as it will produce the optimal set of modulating and demodulating functions to use. The location of noise in the system plays a role in BER, and also dictates whether the diffusivity of the channel affects the BER. This thesis is connected with inverse problems, i.e, our aim is to be able to reconstruct with minimal loss the information we input into the system, x_i, given the information we receive at the ouput, y_i, and the main goal of the work is to derive "sensible choices" of ϕ and $\tilde{\phi}$ to this end.

4 Appendix

This appendix section will give brief summaries over other results obtained throughout my studies, as well as guided information for future models being used and various applicable fields.

4.1 Models and results

4.1.1 Advection-Diffusion Transfer Function

When studying the homogeneous advection-diffusion equation we considered the following solution:

$$h(x-t,t) = \sqrt{\frac{Pe}{4\pi t}} e^{-Pe\frac{(x-t)^2}{4t}} \tag{31}$$

To analyse the behaviour of this solution it is best to plot its behaviour against a change of paramter values (such as velocity, diffusivity, and the distance between transmitter and receiver). In varying these parameters we obtain some of the following figures:

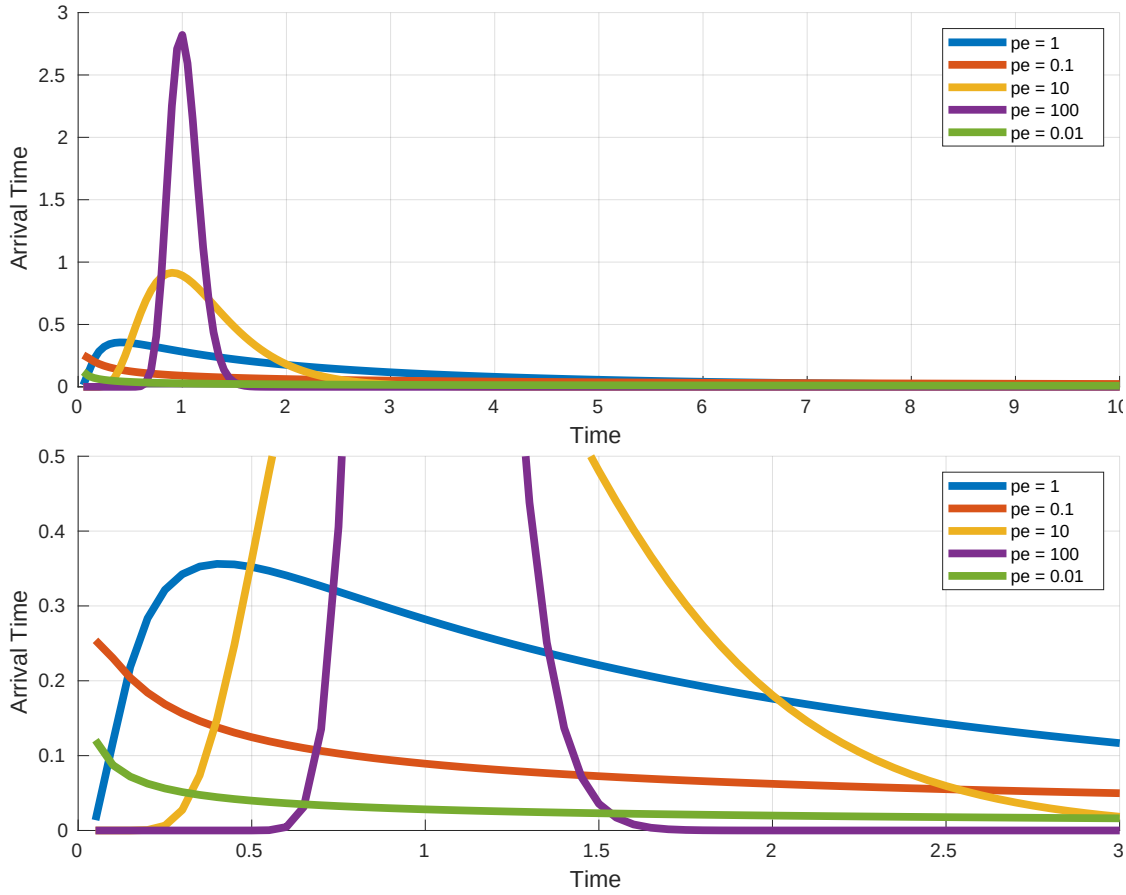

Figure 12: An arrival time distribution showing how particles travel within a fluid flow.

Figure 12 shows the arrival time distribution of our function when the diffusive rate varies but

the velocity of the fluid remains at 1, and the position is taken to be at $x = 1$. It is easy to notice the physical features appearing here because the velocity of the fluid is moving at a rate of 1 unit per second, and since the arrival time is being measured at $x = 1$ then everything happens around 1 second. From a physical interpretation, we would expect that the concentration of the solute would disperse throughout the fluid and not all the solute would be measured at our receiver at the same time, thus resulting in a lower concentration of our solute at the receiver for a large diffusive coefficients, giving an arrival time distribution that is smaller when compared to smaller diffusive coefficients; which is indeed what this figure shows. The larger the diffusive rate the less defined is the peak of the arrival time distribution graph and the smaller the diffusive rate the more defined is the peak of the arrival time distribution graph; this is what the figure shows. This is down to the fact the convective term would be more influential in the fluid and thus the solute would travel mainly by the fluid motion and not its own random Brownian motion given by diffusion, resulting in more of the solute reaching the receiver at the same time.

The zoomed in graph in figure Fig. 12 is to help see the features of the graphs at an earlier time more clearly. From this figure we can see the graphs of the blue, orange, and green lines and see their behaviour better. So it is now easy to notice that when the diffusive term is increased (i.e the Peclet number is decreased since $\text{Pe} \propto \frac{v}{D}$, where v is velocity and D is diffusion) then there is no peak which appears, and this is due to the reasons mentioned above regarding Brownian motion.

Similar figures are plotted to represent this phenomena in Figure (13) whose plots are taken for the same values as the previous figure.

These figures help us in understanding further the behaviour of the particles within the fluid flow. The semi-log figure at the top of Fig. 13 shows how the effects of Brownian motion (i.e large diffusive coefficients) continue to have an effect (relatively) long after the majority of the particles have past through the receptor. For instance, the blue, orange, and green graphs have very long tails (known as breakthrough curves in engineering). These breakthrough curves represent the particles which did not follow the bulk finally passing through the receptor some time later.

The log-log figure at the bottom of Fig. 13 helps show what happens early and late on in time more clearly. Once again if we focus on the blue, orange, and green graphs we see that since the diffusive coefficient is large the is a higher concentration of particles which reach the receptor initially (since they are less restricted by the advective flow of unity), however they the long tails representing the particles trickling through (reasons mentioned above) lasts for a relatively long time (100 seconds); whereas the purple and yellow graphs had all (or if not mostly all) of the particles pass through the receiver within 10 seconds as they were largely influenced by the advective driven term.

So with the help of the figures we can see that the behaviour of the fluid flow is heavily influenced by the advective and diffusive terms, and depending on which term is more powerful will determine the outcome in the arrival time distribution.

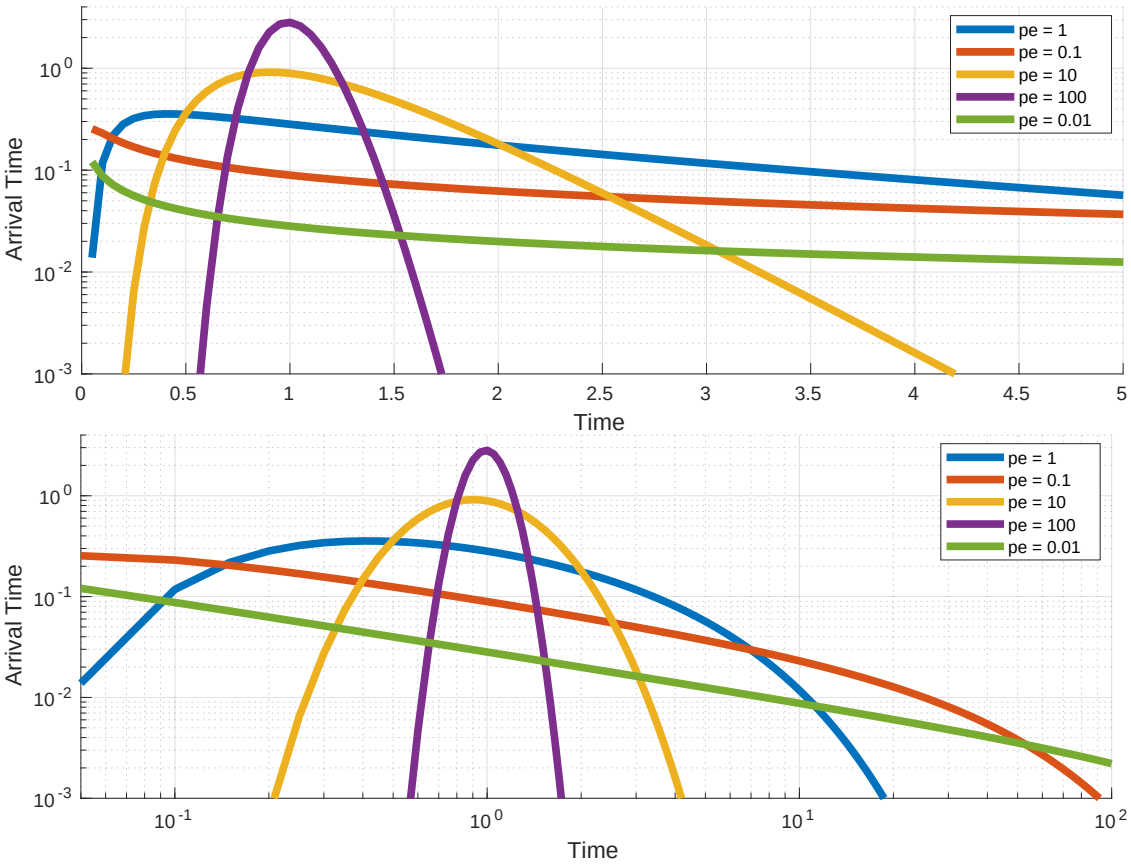

Figure 13: Comparison of arrival time distributions for different velocities and diffusive rates at location $x = 1$.

4.1.2 Mobile-Immbile Transfer Function

The model looks as follows:After studying the advection-diffusion equation we moved on to a more realistic model which involves adds a reaction term along with the advective and diffusive terms, known as the advection-diffusion-reaction equation. The whole model itself consisted of a in-homogeneous advection-diffusion-reaction equation and an ODE which describes the exchange of free flowing particles from the porous medium to particles which get trapped or stuck within the porous medium. The solution we arrived at from studying this model is the following:

$$\tilde{c}(X_R, s) = \sqrt{\frac{\pi}{2\zeta^2(s)}}\, e^{-L\zeta(s)}, \quad \zeta(s) = \sqrt{P^2 + \frac{s\,(s + 2Da)}{(s + Da)}} \tag{32}$$

Where we have the same solution given in (**??**) but in a non-dimensionalised form, with Pe and Da represendting the Peclet and Damkohler numbers.

Once again to analyse the behaviour of the solution we plot multiple figures of it for its varying parameters. In this case the varying parameters are the Peclet number (Pe), defined as the ratio between the velocity and diffusion coefficients, and the Damkohler number (Da), related to the

strength of the mass transfer. Four figures can be seen below. Each figure is plotted using the same varying values, however the axis are scaled differently; one is a linear plot (and a zoomed in version), another a semilog plot, and lastly a loglog plot.

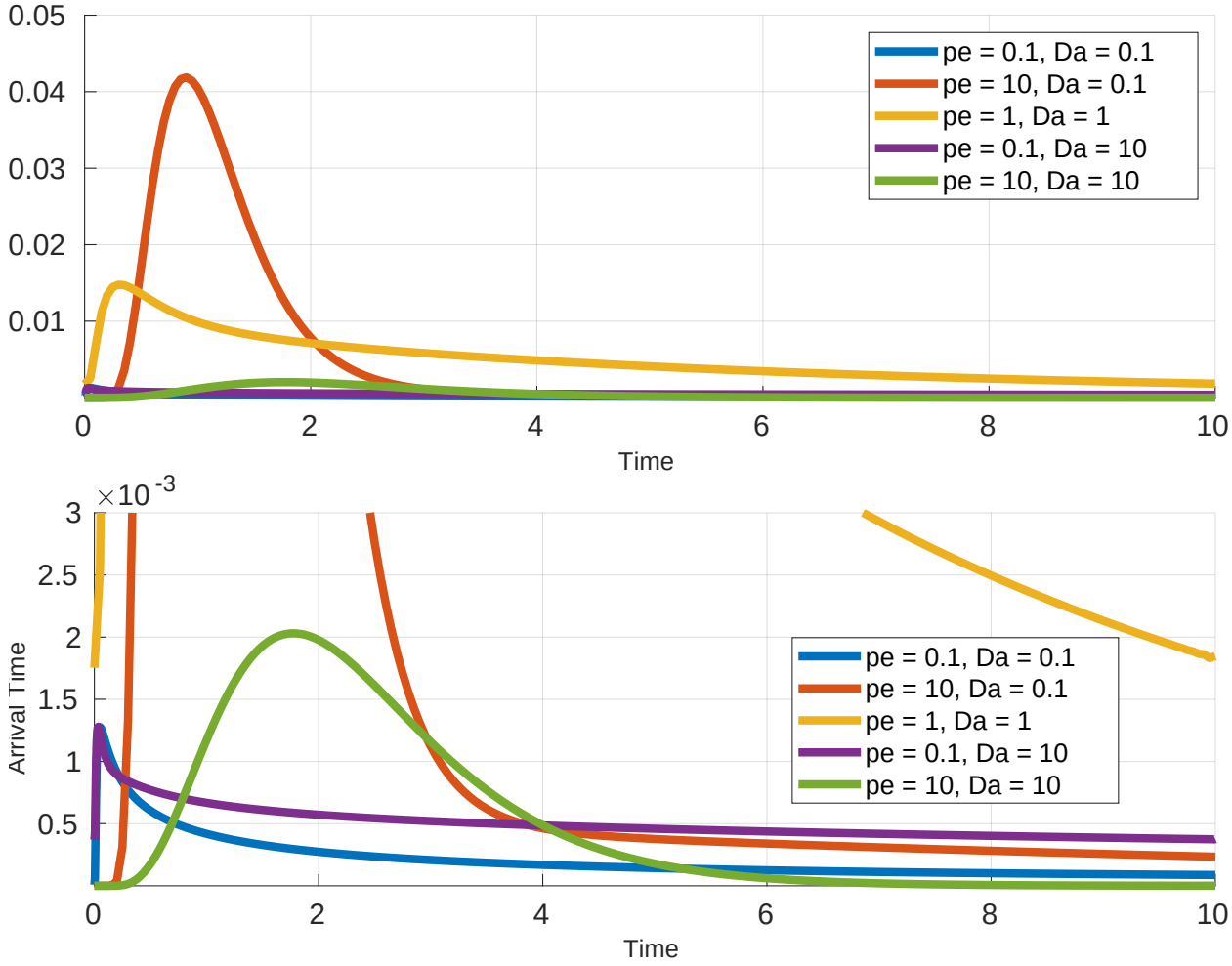

Figure 14: Arrival time distribution with a velocity = 1 and varying values for Pe and Da (left). A zoomed in arrival time distribution with a velocity = 1 and varying values for Pe and Da (right).

What these first two (linearly scaled) figures are showing is the probability distribution of particles travelling through the porous medium. Since the velocity of the system is taken to be equal to 1 and we have parameterised the distance between the transmitter and receiver to also be 1 then we would expect the distribution profile of the particles in the system to be centralised around time equal to 1 (which is what is shown by the figures); i.e the majority of the particles will reach the receiver after one second since the advective term is usually more prominent than the diffusive term and it is set at unity.

However, as can be seen from the figures the distribution profile changes depending on the values given to the parameters Pe (Peclet) and Da (Damkohler). These two parameters define how

strong the diffusive term will be and how strong the exchange rate of particles from the mobile part of the porous medium to the immobile part of the porous medium will be, respectively. So if we increase the value of the Pe number (decrease the power of the diffusive term) we will expect the advective terms to be even more powerful and thus the profile should be even more centralised around 1 second, and if the Pe number is reduced (increase the power of the diffusive term) we will expect there to be a less defined distribution around 1 second (not as prominent a peak). Looking at the figures this is exactly what we see, when the diffusive term is not as significant the peak is larger at 1 second, and when the diffusive term is more significant the peak is smoothed out (due to the random motion of particles travelling in the medium). For the Da number we would expect that increasing its value would result in more particles being trapped and thus having prolonged tails (representing particles reaching the receiver after relatively long periods of time), and reducing its value would result in less particles being trapped and so not as much of defined tails.

The other two figures plotted (Fig. 15) are the semi-log- and log-log- scaled plots respectively. These two figures help us analyse the behaviour of the system by highlighting different features within it.

From the semi-log plot we can see how the particles which have been trapped can have very long lasting effects on the system. For instance if we observe the orange line we see that there is a defined peak around 1 second which represents the vast majority of particles reaching the receptor, but then after around 3-4 seconds we notice a sharp cut off into a very long linearly decreasing tail. This long tail is caused by the particles that have been trapped finally reaching the receptor after being released back into the free moving porous medium. If we compare this graph to the graph of the green line, were the Peclet number is the same but Da number is larger (stronger chance of particles being trapped) then we notice there is not a straight cut off into a long linearly decreasing tail. Instead, we see that the graph ends within 10 seconds and this is due to the fact that there is so little movement of particles within the porous medium due to them being stuck in the immobile part, and so there is a very small amount of particles reaching the receptor. From the log-log plot we observe a different pattern forming. What these figures help show is how the particles are travelling in the early stages as well as the later stages. For instance if we again look at the green graph we notice that it takes a longer time for the vast majority of particles to reach the receptor; in fact compared to the purple graph it is of a factor of around 10^{-14} smaller until around 0.1 seconds in, were then the green graph begins to increase its concentration of particles reaching the receptor. This is down to the fact the purple graph has a small Peclet number (large diffusive coefficient) which means there is a steady concentration of particles reaching the receptor, and not a bulk of particles which is the case when the advective term is more powerful, which is true for the green graph. After around 10 seconds we see the green graph start to dip which means the majority of particles have already reached the receptor.

So, much like the advective-diffusion equation where the advective and diffusive terms drove the physical features of the system, the same applied in the case of the advective-diffusion-reaction model equation, with the addition of the exchange rate term (Da number) also having an impact.

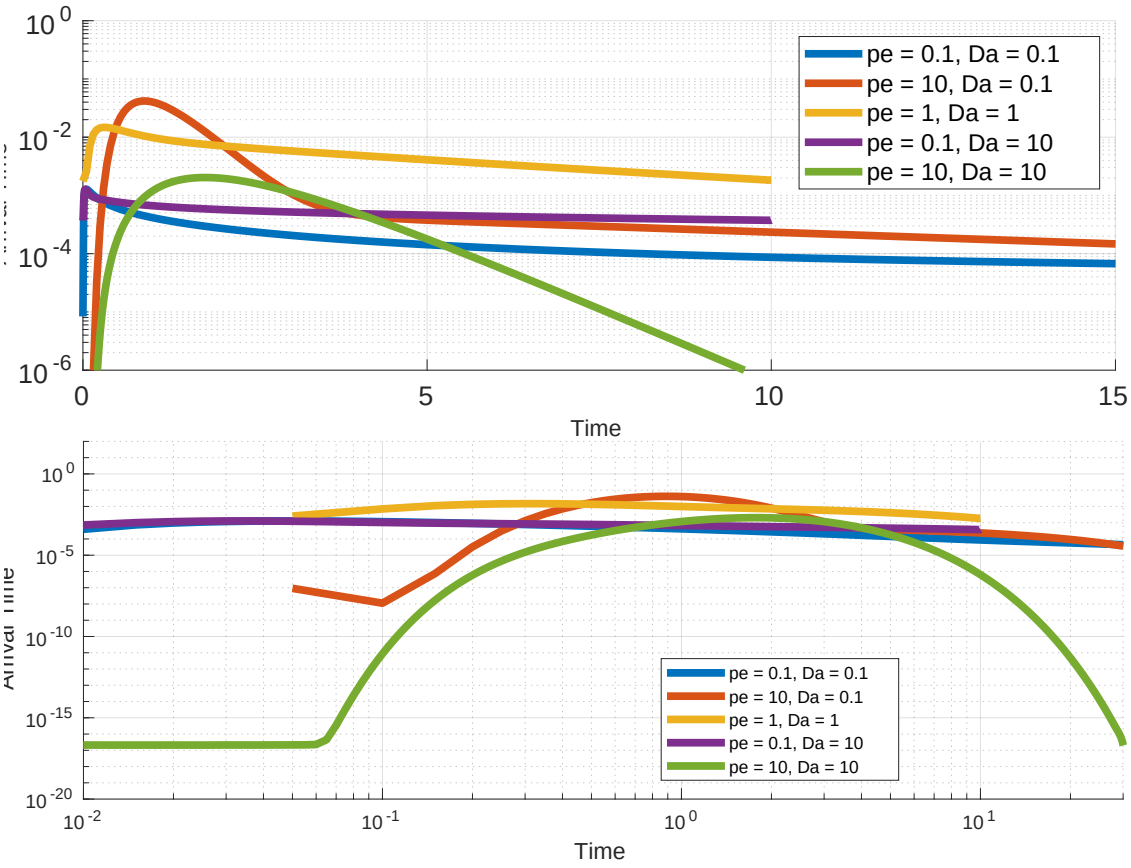

Figure 15: Both figures represent the same transport phenomena in a porous medium but highlight different features, with the top and bottom graphs having semi-log and log-log axes respectively.

So in comparing the two model problems (advection-diffusion model and the immobile-mobile model) we see that they share the same physical properties of the bulk concentration of particles passing the receiver around the same time when the advective term is dominant, and the dispersive nature of the medium when the diffusion term is dominant; with the immobile-mobile model having an additional property of particles being trapped within the porous medium.

4.1.3 Multi-Phase Flow Model

For two mobile phases the model looks as follows:

$$\begin{aligned} Pe_1\frac{\partial c}{\partial t} + Pe_1\frac{\partial c}{\partial x} - \frac{\partial^2 c}{\partial x^2} &= Da_1(b-c) + P(x,t) \\ Pe_2\frac{\partial c}{\partial t} + Pe_2\frac{\partial c}{\partial x} - \frac{\partial^2 c}{\partial x^2} &= Da_2(b-c) + P(x,t) \\ \frac{db}{dt} &= (Da_1 + Da_2)(c-b) \end{aligned} \tag{33}$$

4.1.4 Multi-Rate-Mass-Transfer Model

For two immobile phases the model looks as follows:

$$\begin{aligned} Pe\frac{\partial c}{\partial t} + Pe\frac{\partial c}{\partial x} - \frac{\partial^2 c}{\partial x^2} &= \sum_{i=1}^{2} Da_i(b_i - c) + P \\ \tilde{c}(x, 0; \tau) &= \sum_{i=1}^{2} Da_i \tilde{b}_i + \tilde{P} \\ \frac{\partial b_1}{\partial t} &= Da_1(c - b_1) \\ \frac{\partial b_2}{\partial t} &= Da_2(c - b_2) \end{aligned} \tag{34}$$

An analytical solution of this model is derived in Fourier space and time (refer to 4.2.3).

4.1.5 Towards uncertainty quantification: sensitivity analysis

When wanting to analyse a porous medium it is essential to know the values of the parameters within the system; such as the velocity and diffusion (both associated with the Peclet number), and the mass transfer rate between mobile and immobile regions (associated with the Damkohler number). However, knowing the exact value of these parameters is not realistic and so instead we must look for a range of potential values of these parameters. If we can obtain a sufficient range which makes physical sense for the system in question, and if we have a rough idea of what we are looking for/expecting, then the role of Uncertainty Quantification (UQ) and sensitivity analysis comes in to play.

$$Q = \int_{T-\Delta t}^{T+\Delta t} c(X_R, t)dt \tag{35}$$

What sensitivity analysis does is allow us to obtain an optimal solution for the different values of parameters given. For instance, if we take our mobile-immobile model solution and take the quantity of interest (35) (the feature we are interested in, Q) to be the definite area under the curve (probability of arrival time) between the time units $T - \Delta t$ and $T + \Delta t$ (where T is the peak value of arrival time and Δt is a time step around T), and if we vary the Peclet and Damkohler numbers within a suitable range then we obtain the contour map shown in Fig. 16
The reason for the integration range comes from non-dimensionalising the model problem and normalising the velocity of the system to unity (hence we know the bulk amount of particles should arrive roughly around 1 unit of time). This mapping shows that there is an optimal value for the quantity of interest when the value of the Peclet number is high. What this means is that if the velocity of the porous medium is high then there is a greater probability of the molecules in the porous medium arriving at the receiver in 1 unit of time.

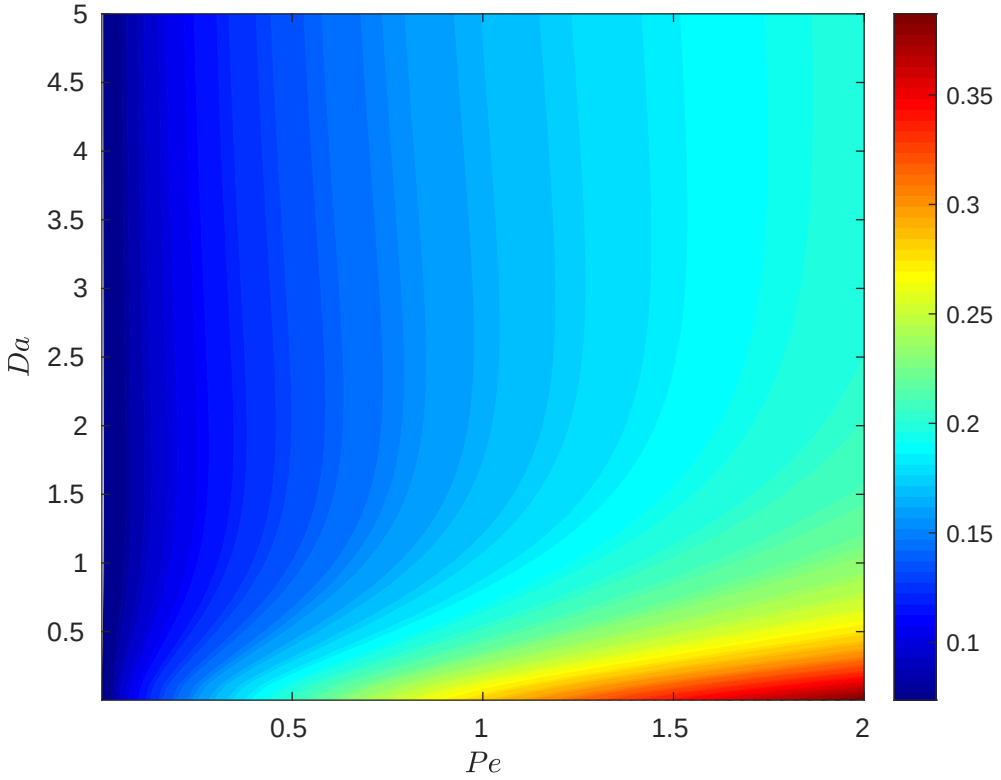

Figure 16: Contour map showing integral of mobile-immobile model solution in the range of 0.5 to 1.5 units of time

4.2 Methods and Proofs

4.2.1 Proof of THM 1

Proof. Proving through direct substitution yields the following:

$$\begin{aligned} y_j &= \sum_{i=1}^{N} x_i \int_0^{\infty} \int_0^{t} \left(\phi_i(t-\tau)h(\tau; x_R, Pe)\right)\, d\tau\, \tilde{\phi}_j(t)\, dt \\ &= \sum_{i=1}^{N} x_i \left(\delta_{ij} + O(\epsilon)\right) \end{aligned} \tag{36}$$

where the identity (10) from Theorem. 1 is used. Subtracting x_j from both sides gives

$$y_j - x_j = \sum_{i=1}^{N} x_i \left(\delta_{ij} + O(\epsilon)\right) - x_j. \tag{37}$$

It is a property of the Kronecker delta function that $\sum_i^N f_i \delta_{ij} = f_j$, and since we are after a single input, $k = i$, we lose the summation and deal strictly with x_j and y_j. we then produce the following error in output:

$$\begin{aligned} y_j - x_j &= x_j + \sum_{i=1}^{N} x_i O(\epsilon) - x_j \\ &= x_j + O(\epsilon) - x_j \\ &= O(\epsilon) \end{aligned} \tag{38}$$

Note that taking the $L1$ norm of this equation is simply just the difference between two points, and so Eq. 38 is equivalent to writing:

$$|y_i - x_i| = O(\epsilon). \tag{39}$$

4.2.2 A procedural approach

The bi-orthogonal approach discussed in section (2.2) is expanded here, with this section dealing with orthogonal functions in general; with the focus of trying to implement a procedure to solve the problem of demodulation – the idea being that the use of an algorithmic type process, based off a proof-by-induction approach, may be suitable to find an optimal solution. One question which has been birthed recently from our research is, "*Can we find a generic function $\tilde{\phi}$ which is bi-orthogonal to a generic modulating function ϕ, which is under a convolution operation with a transfer function h.*"? Mathematically this question is formulated as follows:

$$\int_0^\infty \left[\phi_i(t) * h(x_R, t)\right] \tilde{\phi}_j \, dt = \delta_{ij} \tag{40}$$

where δ_{ij} is the Kronecker delta, x_R represents the location of the receiver, and x is the transmitted signal.

To begin answering this question we will investigate the case where our modulating function (ϕ) is not shifted in time, but is rather a continuous signal being transmitted, as shown by its arguments in 40. Written another way, the problem we want to answer can be short handed to:

$$\left\langle \phi_i, \tilde{\phi}_j \right\rangle_{*h} = \delta_{ij}$$

where the subscript '$*h$' notation denotes the scalar product between the convolution of ϕ_i and h with $\tilde{\phi}_j$.

With the introduction of the convolution operator another question arises: "*Does (40) hold true with this convolution, or is it best written as* $\left\langle \phi_i, \tilde{\phi}_j \right\rangle_{*h} = \delta_{ij} + \epsilon$"? Where ϵ is a small error term. So, we need to investigate if this scalar product is equal to the Kronecker delta under the convolution operation, or if it is more correct to say it is approximately equal to the Kronecker delta.

Assuming $\left\langle \phi_i, \tilde{\phi}_j \right\rangle_{*h} = \delta_{ij}$ then we can try to prove the existence of a solution using proof by induction (of sorts). I.e:

$$\left\langle \phi_1, \tilde{\phi}_1 \right\rangle = 1$$

$$\left\langle \phi_1, \tilde{\phi}_2 \right\rangle = 0$$
$$\left\langle \phi_2, \tilde{\phi}_2 \right\rangle = 1$$
$$\vdots$$

where we have dropped the subscript '$*h$' notation for convenience.

For our first case let's take $\phi_1(t) = \delta(t)$. In this case, for $\left\langle \phi_1, \tilde{\phi}_1 \right\rangle = 1$ to hold we can choose $\tilde{\phi}_1$ to be a constant function (say the Heaviside function). So $\left\langle \phi_1, \tilde{\phi}_1 \right\rangle = 1$ is satisfied. What we have accomplished is effectively the 'switching on' of the first signal (modulated by ϕ) sent; now how do we 'switch off' the signal? To do this we must satisfy $\left\langle \phi_1, \tilde{\phi}_2 \right\rangle = 0$, where $\tilde{\phi}_2$ is the generic function to switch off the first signal sent. Writing the problem out explicitly:

$$\int_0^\infty [\phi_1 * h]\, \tilde{\phi}_2 \, dt = 0 \tag{41}$$

Some algebraic manipulation reduces this equation in the following way:

$$\begin{aligned} \int_0^\infty [\phi_1 * h]\, \tilde{\phi}_2 \, dt &= 0, \quad x \neq 0 \\ \int_0^\infty \left[\phi_1(t) * h(x_R, t)\right] \tilde{\phi}_2(t)\, dt &= 0 \end{aligned} \tag{42}$$

The trivial solution is $\tilde{\phi}_2 = 0$, but this is of no use because this would suggest sending a modulated signal without any external modification, which would not work (as nature will only influence the signal). So if $\tilde{\phi}_2(t) \neq 0$ then we must solve (42).

To move forward let us substitute simple functions (42). we'll keep $\phi_1(t) = \delta(t)$ and take $h(x_R, t)$ to be the inverse Gaussian. Thus, we yield the following equation:

$$\int_0^\infty \left[\delta(t) * \sqrt{\frac{Pe}{4\pi t}} e^{-Pe\frac{(x_R - t)^2}{4t}}\right] \tilde{\phi}_2(t)\, dt = 0 \tag{43}$$

where Pe is the Peclet number. Manipulating this equation yields the following algebra:

$$\begin{aligned} \int_0^\infty \int \left[\delta(t-\tau)\sqrt{\frac{Pe}{4\pi t}} e^{-Pe\frac{(x_R - t)^2}{4t}}\, dt\right] \tilde{\phi}_2(t)\, dt &= 0 \\ \iff \int_0^\infty \left[\sqrt{\frac{Pe}{4\pi \tau}} e^{-Pe\frac{(x_R - \tau)^2}{4\tau}} + a_1\right] \tilde{\phi}_2(t)\, dt &= 0 \\ \iff \left[\sqrt{\frac{Pe}{4\pi \tau}} e^{-Pe\frac{(x_R - \tau)^2}{4\tau}} + a_1\right] \int_0^\infty \tilde{\phi}_2(t)\, dt &= 0 \end{aligned} \tag{44}$$

where a_1 is a constant of integration.

Since we do not know anything about $\tilde{\phi}_2$ we cannot take this any further. however, we can deduce the following can hold:

$$a_1 = -\sqrt{\frac{Pe}{4\pi\tau}} e^{-Pe\frac{(x_R-\tau)^2}{4\tau}}$$

If this holds true then we have obtained a solution to $\left\langle \phi_1, \tilde{\phi}_2 \right\rangle = 0$. However, what we notice is that this identity is not dependent on ϕ_2 but instead depends on the arbitrary constant arising from the convolution of ϕ_1 and h.

The deduction to take from this is summarised in the statement below:

"*If we send a signal from the* ***transmitter*** *modulated by a function which has a certain amplitude and direction, then we can demodulate the signal by sending out a generic function from the* ***receiver*** *which has the same amplitude of the modulating function, but in the opposite direction.*"

By this I claim that if we send a modulating function at time instant t with magnitude A, then we can demodulate this function (without error), obtaining the original signal sent, by sending another signal with the same magnitude, A, but in the opposite direction.

4.2.3 Fourier in time (and space?)

We now move onto a more realistic model known as the multi-rate mass transfer model (MRMTM) (see appendix, 4.1.4). the MRTM is an extension of the mobile-immobile model (MIM) where it encompasses not just one immobile phase but N many immobile phases. We look at the 1D version of this model as done with the ADE model discussed previously, but note we can make the model further realistic by studying its 3D version along with a porosity term; this is studied in the work done by Federico Municchi and Matteo Icardi where they also provide a derivation of the model [39].

The mobile-immobile model is a coupled differential equation consisting of the governing equation (45), which describes the motion of the mobile concentration with a relation to the immobile concentration, and the equation describing the rate of change of the immobile concentration (46).

$$Pe\frac{\partial c}{\partial t} + Pe\frac{\partial c}{\partial x} - \frac{\partial^2 c}{\partial x^2} = \sum_{j=1}^{N} \beta_j (b_j - c) + P \tag{45}$$

$$\begin{aligned} c(x,0) &= 0 \\ \frac{\partial b_j}{\partial t} &= \beta_j (c - b_j) \end{aligned} \tag{46}$$

Looking at (45) we can perform the Fourier Transform on it in time, yielding:

$$Pe\,\frac{1}{2\pi}\int is\,\tilde{c}e^{ist}\,ds + Pe\frac{1}{2\pi}\int \frac{\partial \tilde{c}}{\partial x}e^{ist}\,ds - \frac{1}{2\pi}\int \frac{\partial^2 \tilde{c}}{\partial x^2}e^{ist}\,ds = \tag{47}$$

$$\sum_{j=1}^{N}\beta_j\left(\frac{1}{2\pi}\int b_j e^{ist}\,ds - \frac{1}{2\pi}\int \tilde{c}e^{ist}\,ds\right) + \frac{1}{2\pi}\int Pe^{ist}\,ds \tag{48}$$

$$\tag{49}$$

$\Leftrightarrow$

$$\int\left[\left(Pe\,is + \sum_{j=1}^{N}\beta_j\right)\tilde{c} + Pe\,\frac{\partial \tilde{c}}{\partial x} - \frac{\partial^2 \tilde{c}}{\partial x^2}\right]\,e^{ist}\,ds = \int\left(\tilde{P} + \sum_{j=1}^{N}\beta_j\tilde{b}_j\right)\,e^{ist}\,ds \tag{50}$$

For this equality to be satisfied it must mean the terms within the integrand equate. Thus:

$$\left(Pe\,is + \sum_{j=1}^{N}\beta_j\right)\tilde{c} + Pe\frac{\partial \tilde{c}}{\partial x} - \frac{\partial^2 \tilde{c}}{\partial x^2} = \tilde{P} + \sum_{j=1}^{N}\beta_j\tilde{b}_j \tag{51}$$

Let us look at the PDE describing b_j:

$$\frac{\partial b_j}{\partial t} = \beta_j(b_j - c), \quad j = 1, 2 \tag{52}$$

Using Fourier in time yields:

$$\frac{1}{2\pi}\int is\tilde{b}_j e^{ist}\,ds = \beta_j\left(\frac{1}{2\pi}\int \tilde{b}_j e^{ist}\,ds - \frac{1}{2\pi}\int \tilde{c}e^{ist}\,ds\right) \tag{53}$$

Which can be solved to obtain:

$$\tilde{b}_j = \frac{\beta_j}{\beta_j - is}\tilde{c} \tag{54}$$

Substituting this into (51) gives:

$$\left[Pe\,is + \sum_{j=1}^{N}\left(1 - \frac{\beta_j}{\beta_j - is}\right)\beta_j\right]\tilde{c} + Pe\frac{\partial \tilde{c}}{\partial x} - \frac{\partial^2 \tilde{c}}{\partial x^2} = \tilde{P} \tag{55}$$

For a generic source term $\tilde{P}$ this problem can be solved for our concentration $\tilde{c}$. However, for modulation purposes we choose P to be our carrier function which takes the form of a Dirac delta. This means that trying to solve this PDE for a specific source term $\tilde{P}$ is difficult

To navigate through this mathematical problem we make use of the Fourier Transform in space on (55), yielding:

$$\frac{1}{2\pi}\left[Pe\,is+\sum_{j=1}^{N}\left(1-\frac{\beta_j}{\beta_j-is}\right)\beta_j\right]\int\tilde{\hat{c}}\,e^{ikx}\,dk+\frac{1}{2\pi}Pe\int\tilde{\hat{c}}ik\,e^{ikx}\,dk \tag{56}$$

$$-\frac{1}{2\pi}\int-k^2\tilde{\hat{c}}e^{ikx}\,dk=\frac{1}{2\pi}\int\tilde{\hat{P}}e^{ikx}\,dk \tag{57}$$

Since $e^{ikx}\neq 0$ we reduce this further into its simplest form:

$$\left[Pe(ik+is)-k^2+\sum_{j=1}^{N}\left(1-\frac{\beta_j}{\beta_j-is}\right)\beta_j\right]\tilde{\hat{c}}=\tilde{\hat{P}} \tag{58}$$

Solving explicitly for $\tilde{\hat{c}}$ gives:

$$\tilde{\hat{c}}=\frac{\tilde{\hat{P}}}{Pe(ik+is)-k^2+\sum_{j=1}^{N}\left(1-\frac{\beta_j}{\beta_j-is}\right)\beta_j} \tag{59}$$

We now have an explicit solution of c, with the caveat of it being in Fourier space and time; however this is not necessarily negative as information transfer exists in frequency space too (refer to relevant section here), and so some analysis can be made here.

4.2.4 3D code

An extension of this work is to use existing code developed by my research group to provide figures and simulations of $\tilde{C}$ for every point in space. The aim would then be to apply these results obtained to multiple input multiple output (MIMO) systems. For the time being this is future work and will be investigated at a later date.

4.2.5 Oscillatory channel

Focusing on Eq. 10 we can deduce identities for specific cases of $\phi_i(t)$ and $h(t)$. For instance, in a porous medium which has immobile section for fluid flow, you can observe higher concentrations and lower concentrations of information passing through at different times, due to retention of the information within these immobile sections of the porous medium, creating an oscillatory feature of the information transfer. This oscillatory case $h(t)=sin(kt)$, for some $k\in\mathcal{R}$ we show to have the following identity:

$$\begin{aligned}\int_0^\infty \sin(k(t-T_i))\tilde{\phi}_j(t)\,dt &= -\frac{1}{k}[\cos(k(t-T_i))\tilde{\phi}_j(t)]_0^\infty+\frac{1}{k}\int_0^\infty\cos(k(t-T_i))\tilde{\phi}_j'(t)\,dt\\ &= -\frac{1}{k}[\cos(k(t-T_i))\tilde{\phi}_j(t)]_0^\infty+\frac{1}{k^2}[\sin(k(t-T_i))\tilde{\phi}_j'(t)]_0^\infty-\\ &\frac{1}{k^2}\int_0^\infty\sin(k(t-T_i))\tilde{\phi}_j''(t)\,dt\\ &= \delta_{ij}+O(\epsilon)\end{aligned}$$

Taking some large value $R >> 1$ as $R \to \infty$ and multiplying by k^2 we obtain the following:

$$-\int_{-T_i}^{R} \sin(k\tau)\tilde{\phi}_j''(\tau + T_i)\, d\tau + [\sin(k\tau)\tilde{\phi}_j'(\tau + T_i) - k\cos(k\tau)\tilde{\phi}_j(\tau + T_i)]_0^R = k^2(\delta_{ij} + O(\epsilon)) \quad (60)$$

where $\tau = t - T_i$. Doing this calculation explicitly, under the assumption $\tilde{\phi}_j(t) \to 0$ as $t \to \infty$, we have:

$$\begin{aligned} -\int_{-T_i}^{R} \sin(k\tau)\tilde{\phi}_j''(\tau + T_i)\, d\tau + \sin(kR)\tilde{\phi}_j'(R + T_i) - \sin(-kT_i)\tilde{\phi}_j'(0) - k\cos(kR)\tilde{\phi}_j(R + T_i) \\ + k\cos(-kT_i)\tilde{\phi}_j(0) \\ = -\int_{-T_i}^{R} \sin(k\tau)\tilde{\phi}_j''(\tau + T_i)\, d\tau + \big(\sin(kR) + \sin(kT_i)\big)\,\tilde{\phi}_j'(0) \\ - k\,\big(\cos(kR) - \cos(kT_i)\big)\,\tilde{\phi}_j(0) \end{aligned}$$

If $\tau = \frac{n\pi}{k}$, $R = \frac{m\pi}{k}$, $T_i = \frac{i\pi}{k}$, with $n = i = 1, 2, ..., m$, where $m \in N$ and $m >> 1$, then we have:

$$-k\,\big(\cos(m\pi) - \cos(i\pi)\big)\,\tilde{\phi}_j(0) = k^2(\delta_{ij} + O(\epsilon)) \quad (61)$$

which then yields:

$$\tilde{\phi}_j(0) = \frac{k(\delta_{ij} + O(\epsilon))}{\cos(i\pi) - \cos(m\pi)} \quad (62)$$

setting $i = j$ results in:

$$\tilde{\phi}_i(0) = \frac{k(1 + O(\epsilon))}{\cos(i\pi) - \cos(m\pi)} \quad (63)$$

That is our demodulating function is

$$\tilde{\phi}_j(0) = \frac{k}{\cos(i\pi) - \cos(m\pi)} \quad (64)$$

with some error $\frac{O(\epsilon)}{\cos(i\pi) - \cos(m\pi)}$ of order ϵ.

Taking instead $\tau = \frac{n\pi}{2k}$, $R = \frac{m\pi}{2k}$, and $T_i = \frac{i\pi}{2k}$ with $n = i = 1, 2, ..., m$ then we have:

$$-\int_{-T_i}^{R} \sin(\frac{n\pi}{2})\tilde{\phi}_j''(\frac{(n+i)\pi}{2k})\, d\tau + \left(\sin(\frac{m\pi}{2}) + \sin(\frac{i\pi}{2})\right)\tilde{\phi}_j'(0) = k^2(\delta_{ij} + O(\epsilon)) \quad (65)$$

What is clear is that the function $\tilde{\phi}_j(0)$ evaluated at zero is dependant on the cosine function. However, its derivatives at zero are dependant on the sine function. That is the rate at which $\tilde{\phi}_j(0)$ changes corresponds to a phase shift of the sinusoidal functions.

4.2.6 Expansion of $\tilde{\phi}_j$

Take

$$\int_0^T \sum_{i=1}^{N} \sin(k(t-T_i))\tilde{\phi}_j(t)\,dt = \delta_{ij} \tag{66}$$

where we now expand $\tilde{\phi}_j$ as a sum of sinusoidal functions

$$\tilde{\phi}_j(t) = \frac{a_0}{2} + \sum_{j=1}^{N} a_j \sin(kt) + b_j \cos(kt). \tag{67}$$

Substituting this (67) into (66) and setting $T = T_i + \frac{2\pi}{k}$ gives the following

$$\int_{T_i-\frac{\pi}{k}}^{T_i+\frac{\pi}{k}} \left(\sum_{i=1}^{N} \sin(k(t-T_i))[\frac{a_0}{2} + \sum_{j=1}^{N} a_j \sin(kt) + b_j \cos(kt)] \right) dt = \delta_{ij} \tag{68}$$

where we integrate over one full period around T_i. Setting $i = j \neq 0$ and expanding out through use of trigonometric identities yields:

$$\int_{T_i-\frac{\pi}{k}}^{T_i+\frac{\pi}{k}} \frac{a_i a_0}{2} \sin(k(t-T_i)) + a_i^2 \left(\sin^2(kt)\cos(kT_i) - \sin(kT_i)\cos(kt) \right) + a_i b_i \left(\sin(kt)\cos(kt)\cos(kT_i) - \sin(kT_i)\cos^2(kt) \right) dt = 1$$

where we can simplify further through orthogonality identities, resulting in:

$$\int_{T_i-\frac{\pi}{k}}^{T_i+\frac{\pi}{k}} \frac{a_i a_0}{2} \sin(k(t-T_i)) + a_i^2 \cos(kT_i) - a_i b_i \sin(kT_i)\,dt = 1. \tag{69}$$

Performing the integral gives:

$$\begin{aligned} 1 &= \left[-\frac{a_i a_0}{2k} \cos(k(t-T_i)) + a_i^2 \cos(kTi)t - a_i b_i \sin(kT_i)t \right]_{T_i-\frac{\pi}{k}}^{T_i+\frac{\pi}{k}} \\ &= -\left(1-\cos(kT_i)\right)\frac{a_i a_0}{2k} + \left(a_i^2 \cos(kT_i) - a_i b_i \sin(kT_i) \right)(T_i + \frac{2\pi}{k}) \end{aligned} \tag{70}$$

Setting different values for T_i will yield relationships between a_i and a_0.

Taking $i \neq j$ and referring back to Eq. 68 yields:

Instead now take $\tilde{\phi}_j$ to be piece-wise linear such that

$$\tilde{\phi}_j(t) = \begin{cases} A_1 t + B_1, & \text{in } t \in [T_1, T_2]. \\ . \\ . \\ . \\ A_l t + B_l, & \text{in } t \in [T_l, T_l + 1] \end{cases} \tag{71}$$

In order to satisfy the continuity of $\tilde{\phi}_j$ we must enforce

$$A_l t_{l+1} + B_l = A_{l+1} t_{l+1} + B_{l+1}. \tag{72}$$

This condition makes the curve piece-wise linear. Re-arranging we can obtain the following:

$$B_{l+1} = B_l + (A_l - A_{l+1}) t_{l+1} \tag{73}$$

If we take N piece-wise linear curves then we have N equations. Substituting into (66) gives:

$$\begin{aligned}
\sum_{l=1}^{N} \int_{T_l}^{T_{l+1}} \sin(k(t - T_i)) \left(A_l t + B_l\right) &= -\frac{1}{k} [\cos(k(t - T_i)) \left(A_l t + B_l\right)]_{T_l}^{T_{l+1}} \\
&+ \frac{1}{k} \int_{T_l}^{T_{l+1}} \cos(k(t - T_i)) \left(A_l t + B_l\right)' \, dt \\
&- \frac{1}{k} [\cos(k(t - T_i)) \left(A_l t + B_l\right)]_{T_l}^{T_{l+1}} + \frac{1}{k} \int_{T_l}^{T_{l+1}} \cos(k(t - T_i)) A_l \, dt \\
&= \sum_{l=1}^{N} -\frac{1}{k} [\cos(k(t - T_i)) \left(A_l t + B_l\right)]_{T_l}^{T_{l+1}} \\
&+ \sum_{l=1}^{N} \frac{1}{k} \int_{T_l}^{T_{l+1}} \cos(k(t - T_i)) A_l \, dt \\
&= \sum_{l=1}^{N} -\frac{1}{k^2} \left([\sin(k(t - T_i)) A_l - k \cos(k(t - T_i)) (A_l t + B_l)]_{T_l}^{T_{l+1}} \right) - \\
&\sum_{l=1}^{N} \int_{T_l}^{T_{l+1}} \sin(k(t - T_i)) * 0 \, dt \\
&= \sum_{l=1}^{N} \left(-\frac{1}{k^2} \left([\sin(k(t - T_i)) A_l - k \cos(k(t - T_i)) (A_l t + B_l)]_{T_l}^{T_{l+1}}) \right) \right) \\
&= \delta_{ij}
\end{aligned}$$

4.3 Singular Value Decomposition

SVD is a mathematical tool which allows for the factorisation of any generic matrix into three other matrices. These matrices are factorised in such a way that as we move along its columns the entries become less important compared to the earlier columns. This is what allows for nice approximations to be made as we are able to omit some (if not most) of the SVD matrix, and still yield very approximate results.

For instance, if we take our transfer matrix $\mathbf{H}$ we are able to factorise it into its SVD form, which is given to be:

$$\mathbf{H}_{p\times q} = \mathbf{U}_{p\times p}\mathbf{\Sigma}_{p\times q}\mathbf{V^T}_{q\times q} = \begin{bmatrix} . & . & . & . & . & . \\ . & . & . & . & . & . \\ . & . & . & . & . & . \\ U_1 & U_2 & . & . & . & U_p \\ . & . & . & . & . & . \\ . & . & . & . & . & . \end{bmatrix} \begin{bmatrix} \sigma_1 & . & . & . & . & . & . \\ . & \sigma_2 & . & . & . & . & . \\ . & . & . & . & . & . & . \\ . & . & . & . & . & . & . \\ . & . & . & . & . & . & . \\ . & . & . & . & . & . & \sigma_q \end{bmatrix} \begin{bmatrix} . & . & . & . & . & . \\ . & . & . & . & . & . \\ . & . & . & . & . & . \\ V_1^T & V_2^T & . & . & . & V_q^T \\ . & . & . & . & . & . \\ . & . & . & . & . & . \end{bmatrix} \tag{74}$$

where $\mathbf{U}$ is a *pxp* unitary matrix, $\mathbf{\Sigma}$ is a *pxq* singular diagonal matrix, and $\mathbf{V^T}$ is a *qxq* unitary matrix. The singular matrix is ordered in such a way that $\sigma_1 > \sigma_2 > ... > \sigma_q$, giving rise to what we call *order of importance*. This ordering is what causes the earlier columns of the unitary matrices to be more *important* (or prevalent) in capturing the processes of the system. However, working with this full SVD is not idea and so the creation of reduced SVD's were introduced to make this tool more appropriate for certain situations.

4.3.1 Reduced SVD

It is often inconvenient to use the full SVD as it uses excess computational power than is actually needed for solving most problems. In order to be cost efficient with regards to computational power there are multiple ways to reduce the SVD and still yield exact or approximate solutions. The first reduced SVD we will discuss is what is commonly referred to as the *econ* SVD (or *thin* SVD). It is defined as the following:

$$\mathbf{H}_{p\times q} = \hat{\mathbf{U}}_{p\times q}\hat{\mathbf{\Sigma}}_{qxq}\mathbf{V^T}_{qxq} = \begin{bmatrix} . & . & . & . & . & . \\ . & . & . & . & . & . \\ . & . & . & . & . & . \\ U_1 & U_2 & . & . & . & U_q \\ . & . & . & . & . & . \\ . & . & . & . & . & . \end{bmatrix} \begin{bmatrix} \sigma_1 & . & . & . & . & . \\ . & \sigma_2 & . & . & . & . \\ . & . & . & . & . & . \\ . & . & . & . & . & . \\ . & . & . & . & . & . \\ . & . & . & . & . & \sigma_q \end{bmatrix} \begin{bmatrix} . & . & . & . & . & . \\ . & . & . & . & . & . \\ . & . & . & . & . & . \\ V_1^T & V_2^T & . & . & . & V_q^T \\ . & . & . & . & . & . \\ . & . & . & . & . & . \end{bmatrix} \tag{75}$$

where the dimensionality of the left matrix reduces, along with the dimensionality of the singular matrix. This reduction in dimension is due to only the non-zero entries of the singular matrix $\mathbf{\Sigma}$

being considered, and is denoted by the $\hat{}$ notation. This means that the rest of the matrix is omitted and thus the dimension of $\mathbf{U}$ reduces (multiplication by zero yields nothing). Thus we end up with the reduced SVD Eq. (75), which remains exactly equal to $\mathbf{H}$.

In some cases, such as the case this report deals with, it is convenient to further reduce the SVD matrix. In doing so, the SVD is no longer exactly equal to $\mathbf{H}$ but instead is an approximation of it. This is because this further reduced SVD (known as the truncated SVD) takes only the first r columns of $\mathbf{U}$ ($r << p$), first r block of $\mathbf{\Sigma}$, and r columns of $\mathbf{V^T}$.

$$\mathbf{H}_{p\times q} \approx \mathbf{H}_{p\times r} = \tilde{\mathbf{U}}_{p\times r}\hat{\mathbf{\Sigma}}_{rxr}\mathbf{V^T}_{rxr} = \begin{bmatrix} . & . & . & . & . & . \\ . & . & . & . & . & . \\ . & . & . & . & . & . \\ U_1 & U_2 & . & . & . & U_r \\ . & . & . & . & . & . \\ . & . & . & . & . & . \end{bmatrix} \begin{bmatrix} \sigma_1 & . & . & . & . & . & . \\ . & \sigma_2 & . & . & . & . & . \\ . & . & . & . & . & . & . \\ . & . & . & . & . & . & . \\ . & . & . & . & . & . & . \\ . & . & . & . & . & . & . \\ . & . & . & . & . & . & \sigma_r \end{bmatrix} \begin{bmatrix} . & . & . & . & . & . \\ . & . & . & . & . & . \\ . & . & . & . & . & . \\ V_1^T & V_2^T & . & . & . & V_r^T \\ . & . & . & . & . & . \\ . & . & . & . & . & . \end{bmatrix} \tag{76}$$

Where the truncated SVD is denoted by the $\tilde{}$ notation. This truncation of the first r columns relates to the truncation of the first m modes (or symbols) of our signal. How approximate this truncated SVD is in capturing the features of the modulation process depends on how many symbols we take into consideration. The more symbols we take the more accurate the approximation becomes. As an illustrative example we can take the image of H and plot it as follows:

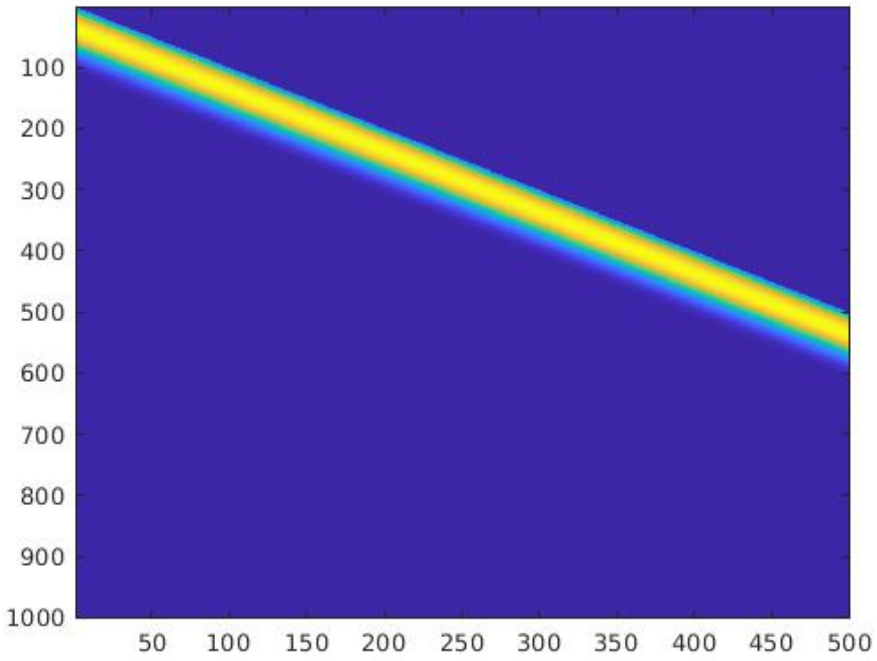

Figure 17: This is the 'image' of the Toeplitz transfer matrix H.

This is the image produced when plotting the Toeplitz transfer matrix in MATLAB using the *imagesc* command. To compare the efficiency of the SVD and truncated SVD we will use the same command to plot these images for varying values of our symbol parameter m. The result is shown below:

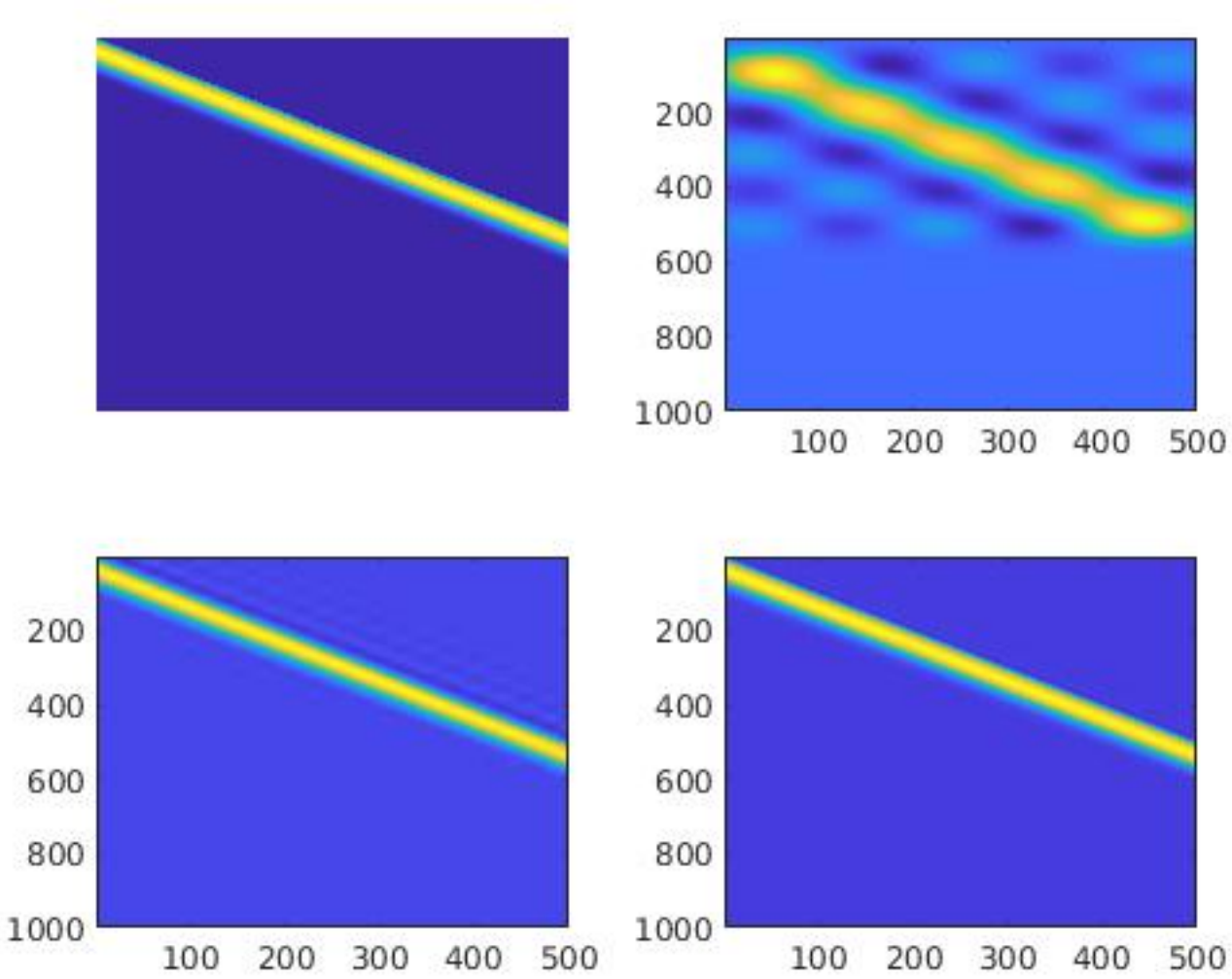

Figure 18: This is the SVD and truncated SVD for varying parameter values of $m = 5, 20, 50$, out of a total of 500 possible symbols.

It is cleat that as we increase the number of symbols we get a closer approximation to the original H. To give some quantitative values it is useful to plot singular values of the matrix $\mathbf{\Sigma}$ and the cumulative energy values for increasing number of symbols. The results are shown below:

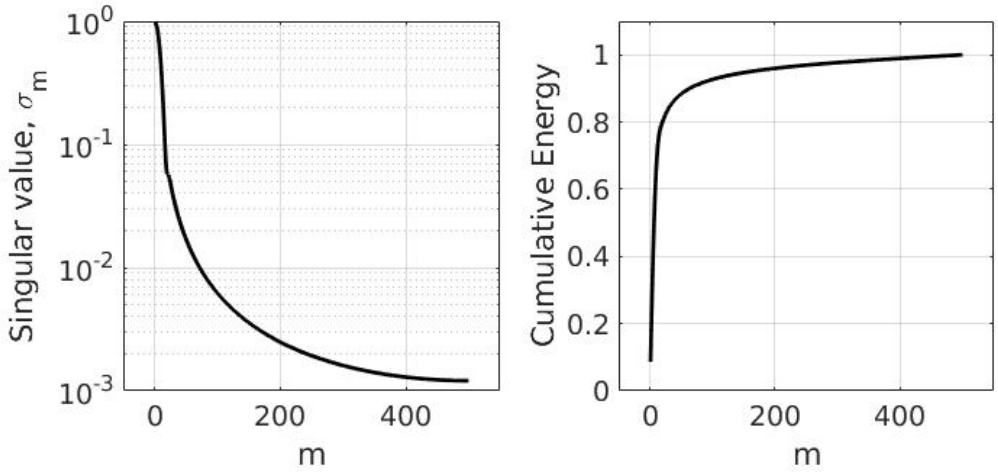

Figure 19: The singular values of the matrix $\mathbf{\Sigma}$ are plotted on the left to show the more dominant entries in the matrix. The cumulative energy is plotted on the right, showing the amount of energy captured by the SVD approximation depending on the number of symbols used.

It is clear to see that the most dominant terms in the singular matrix are captured in the first few symbols, and thus we can justify omitting the latter symbols as they are not as '*important*' in capturing the features of the system. When observing the cumulative energy plot is also clear that as we increase the number of symbols used we approach the total energy of the system, which is to be expected. This is because as we keep increasing the number of symbols used, we are approaching the total number of symbols used (500 in this case), which would effectively be the full SVD. What both these plots show is that the number of symbols needed to use to get a good approximation of the system is not many. In fact, the cumulative energy plot shows that only a fraction of the symbols are required to achieve a high energy output. So now the question becomes how do we quantify good? I believe the next step here is to use principal component analysis (PCA), which provides a hierarchical system for our modulating and demodulating functions. This allows for a more rigid statistical analysis/interpretation of the work done so far using just solely SVD, opening up a data driven approach to be explored in the future.

References

[1] Scott Hayes, Celso Grebogi, and Edward Ott. "Communicating with chaos". In: *Phys. Rev. Lett.* 70 (20 May 1993), pp. 3031–3034. DOI: 10.1103/PhysRevLett.70.3031. URL: https://link.aps.org/doi/10.1103/PhysRevLett.70.3031.

[2] John C Pederson and Timothy J Vogt. *Network security and variable pulse wave form with continuous communication*. US Patent 9,455,783. Sept. 2016.

[3] Timothy J Crish, James D Sweeney, and J Thomas Mortimer. *Antidromic pulse generating wave form for collision blocking*. US Patent 4,608,985. Sept. 1986.

[4] William H Berkman, David Stanley Yaney, and James Douglas Mollenkopf. *Surface wave power line communications system and method*. US Patent 7,280,033. Oct. 2007.

[5] Zhouyue Pi and Farooq Khan. "An introduction to millimeter-wave mobile broadband systems". In: *IEEE communications magazine* 49.6 (2011), pp. 101–107.

[6] Nariman Farsad et al. "A comprehensive survey of recent advancements in molecular communication". In: *IEEE Communications Surveys & Tutorials* 18.3 (2016), pp. 1887–1919.

[7] Weisi Guo et al. "Molecular versus electromagnetic wave propagation loss in macro-scale environments". In: *IEEE Transactions on Molecular, Biological and Multi-Scale Communications* 1.1 (2015), pp. 18–25.

[8] Milica Stojanovic. "Acoustic (underwater) communications". In: *Wiley Encyclopedia of Telecommunications* (2003).

[9] Ian F Akyildiz, Fernando Brunetti, and Cristina Blázquez. "Nanonetworks: A new communication paradigm". In: *Computer Networks* 52.12 (2008), pp. 2260–2279.

[10] Tadashi Nakano, Andrew W Eckford, and Tokuko Haraguchi. *Molecular communication*. Cambridge University Press, 2013.

[11] Tatsuya Suda et al. "Exploratory research on molecular communication between nanomachines". In: *Genetic and Evolutionary Computation Conference (GECCO), Late Breaking Papers*. Vol. 25. 2005, p. 29.

[12] P-L Lions and TH Moulden. "Mathematical topics in fluid mechanics, Volume 1: Incompressible models". In: *APPLIED MECHANICS REVIEWS* 50 (1997), B81–B81.

[13] Pierre-Louis Lions. *Mathematical Topics in Fluid Mechanics: Volume 2: Compressible Models*. Vol. 2. Oxford University Press on Demand, 1996.

[14] Y. Chahibi et al. "A Molecular Communication System Model for Particulate Drug Delivery Systems". In: *IEEE Transactions on Biomedical Engineering* 60.12 (2013), pp. 3468–3483.

[15] David A Lavan, Terry McGuire, and Robert Langer. "Small-scale systems for in vivo drug delivery". In: *Nature biotechnology* 21.10 (2003), pp. 1184–1191.

[16] Mehmet Sukru Kuran, Tuna Tugcu, and Bilge Ozerman Edis. "Calcium signaling: Overview and research directions of a molecular communication paradigm". In: *IEEE Wireless Communications* 19.5 (2012), pp. 20–27.

[17] Massimiliano Pierobon and Ian F Akyildiz. "A physical end-to-end model for molecular communication in nanonetworks". In: *IEEE Journal on Selected Areas in Communications* 28.4 (2010), pp. 602–611.

[18] Ian F Akyildiz, Josep Miquel Jornet, and Massimiliano Pierobon. "Nanonetworks: A new frontier in communications". In: *Communications of the ACM* 54.11 (2011), pp. 84–89.

[19] Ping-Cheng Yeh et al. "A new frontier of wireless communication theory: diffusion-based molecular communications". In: *IEEE Wireless Communications* 19.5 (2012), pp. 28–35.

[20] Weisi Guo et al. "Molecular communications: Channel model and physical layer techniques". In: *IEEE Wireless Communications* 23.4 (2016), pp. 120–127.

[21] Kamal Darchini and Attahiru S Alfa. "Molecular communication via microtubules and physical contact in nanonetworks: A survey". In: *Nano Communication Networks* 4.2 (2013), pp. 73–85.

[22] Tadashi Nakano et al. "Molecular communication among biological nanomachines: A layered architecture and research issues". In: *IEEE transactions on nanobioscience* 13.3 (2014), pp. 169–197.

[23] Sasitharan Balasubramaniam et al. "A review of experimental opportunities for molecular communication". In: *Nano Communication Networks* 4.2 (2013), pp. 43–52.

[24] Roy Haggerty and Steven M Gorelick. "Modeling mass transfer processes in soil columns with pore-scale heterogeneity". In: *Soil Science Society of America Journal* 62.1 (1998), pp. 62–74.

[25] Gerald Matz, Helmut Bolcskei, and Franz Hlawatsch. "Time-frequency foundations of communications: Concepts and tools". In: *IEEE Signal Processing Magazine* 30.6 (2013), pp. 87–96.

[26] Claude E Shannon. "Communication in the presence of noise". In: *Proceedings of the IEEE* 72.9 (1984), pp. 1192–1201.

[27] M. N. Khan and W. G. Cowley. "Signal dependent Gaussian noise model for FSO communications". In: *2011 Australian Communications Theory Workshop*. 2011, pp. 142–147.

[28] R. J. Webster. "Ambient noise statistics". In: *IEEE Transactions on Signal Processing* 41.6 (1993), pp. 2249–2253.

[29] C. L. Nikias and J. M. Mendel. "Signal processing with higher-order spectra". In: *IEEE Signal Processing Magazine* 10.3 (1993), pp. 10–37.

[30] F. De Smedt and P.J. Wierenga. "Mass transfer in porous media with immobile water". In: *Journal of Hydrology* 41.1 (1979), pp. 59–67. ISSN: 0022-1694. DOI: https://doi.org/10.1016/0022-1694(79)90105-7. URL: http://www.sciencedirect.com/science/article/pii/0022169479901057.

[31] Wayan Wicke et al. "Modeling duct flow for molecular communication". In: *2018 IEEE Global Communications Conference (GLOBECOM)*. IEEE. 2018, pp. 206–212.

[32] "Nonlinear diffusion and discrete maximum principle for stabilized Galerkin approximations of the convectionGalerkin method, Convectiondiffusion-reaction equations. We derive nonlinear streamline and cross-wind diffusion methods that guarantee a discrete maximum principle for strictly acute meshes and first order polynomial interpolation. For pure convectiondiffusion-reaction problems, two methods are considered: residual based, isotropic diffusion and the previous nonlinear cross-wind diffusion factor supplemented by additional isotropic diffusion scaling as the square of the mesh size. Practical versions of the present methods suitable for numerical implementation are compared to previous discontinuity capturing schemes lacking theoretical justification. Numerical results are investigated in terms of both solution quality (violation of maximum principle, smearing of internal layers) and computational costs." In: ().

[33] U. A. K. Chude-Okonkwo. "Diffusion-controlled enzyme-catalyzed molecular communication system for targeted drug delivery". In: *2014 IEEE Global Communications Conference*. 2014, pp. 2826–2831.

[34] V. Jamali et al. "Channel Modeling for Diffusive Molecular Communication—A Tutorial Review". In: *Proceedings of the IEEE* 107.7 (2019), pp. 1256–1301.

[35] Ke Liu, T. Kadous, and A. M. Sayeed. "Orthogonal time-frequency signaling over doubly dispersive channels". In: *IEEE Transactions on Information Theory* 50.11 (2004), pp. 2583–2603.

[36] P. Raviteja et al. "Interference Cancellation and Iterative Detection for Orthogonal Time Frequency Space Modulation". In: *IEEE Transactions on Wireless Communications* 17.10 (2018), pp. 6501–6515.

[37] W. Kozek and A. F. Molisch. "Nonorthogonal pulseshapes for multicarrier communications in doubly dispersive channels". In: *IEEE Journal on Selected Areas in Communications* 16.8 (1998), pp. 1579–1589.

[38] Mehmet Şükrü Kuran et al. "Energy model for communication via diffusion in nanonetworks". In: *Nano Communication Networks* 1.2 (2010), pp. 86–95.

[39] Federico Municchi and Matteo Icardi. "Macroscopic models for filtration and heterogeneous reactions in porous media". In: *Advances in Water Resources* (2020), p. 103605.

[40] Federico Municchi and Matteo Icardi. "Generalized multirate models for conjugate transfer in heterogeneous materials". In: *Physical Review Research* 2.1 (2020), p. 013041.

[41] M. Rakus, T. Palenik, and J. Dobos. "Measurement of pulse-combining processing gain of UWB communication system using TIMS". In: *2015 38th International Conference on Telecommunications and Signal Processing (TSP)*. 2015, pp. 1–5. DOI: 10.1109/TSP.2015.7296380.

[42] E. Basar. "Transmission Through Large Intelligent Surfaces: A New Frontier in Wireless Communications". In: *2019 European Conference on Networks and Communications (EuCNC)*. 2019, pp. 112–117. DOI: 10.1109/EuCNC.2019.8801961.

[43] J. Y. Dai et al. "Realization of Multi-Modulation Schemes for Wireless Communication by Time-Domain Digital Coding Metasurface". In: *IEEE Transactions on Antennas and Propagation* 68.3 (2020), pp. 1618–1627. DOI: 10.1109/TAP.2019.2952460.

[44] L. B. Stotts et al. “Hybrid Optical RF Airborne Communications”. In: *Proceedings of the IEEE* 97.6 (2009), pp. 1109–1127. DOI: 10.1109/JPROC.2009.2014969.

[45] N. Jain and A. Banerjee. “On Performance Analysis and Code Design for Visible Light Communication”. In: *2019 57th Annual Allerton Conference on Communication, Control, and Computing (Allerton)*. 2019, pp. 536–543. DOI: 10.1109/ALLERTON.2019.8919764.

[46] Na-Rae Kim and Chan-Byoung Chae. “Novel modulation techniques using isomers as messenger molecules for nano communication networks via diffusion”. In: *IEEE Journal on Selected Areas in Communications* 31.12 (2013), pp. 847–856.

[47] N. Kim, A. W. Eckford, and C. Chae. “Symbol Interval Optimization for Molecular Communication With Drift”. In: *IEEE Transactions on NanoBioscience* 13.3 (2014), pp. 223–229.

[48] Nariman Farsad, Weisi Guo, and Andrew W Eckford. “Tabletop molecular communication: Text messages through chemical signals”. In: *PloS one* 8.12 (2013), e82935.